Supporting Information for

Quantification of the IVCT and their structure dependence in a cofacial metal-organic framework

Eleanor R. Kearns,[a,b] Bun Chan,[c] Hunter J. Windsor,[b,] William Lewis,[d] and Deanna M. D'Alessandro[a,b]*

---

[a] *School of Chemical & Biomolecular Engineering, Faculty of Engineering, The University of Sydney, New South Wales, 2006, Australia.*
[b] *School of Chemistry, Faculty of Science, The University of Sydney, New South Wales, 2006, Australia.*
[c] *Graduate School of Engineering, Nagasaki University, Bunkyo 1-14, Nagasaki 852-8521, Japan*
[d] *Sydney Analytical Core Research Facility, The University of Sydney, New South Wales, 2006, Australia.*

*Email: deanna.dalessandro@sydney.edu.au

Experimental

General Methods

Solution-state ^{1}H and ^{13}C NMR spectra were recorded on a Bruker AVANCEIII 300 MHz spectrometer at 298 K. Deuterated solvents were obtained from Cambridge Stable Isotopes and were used as received with the chemical shifts (d) referenced internally to the residual solvent resonances and quoted in ppm. PXRD data were collected with a PANanalytical X'Pert PRO diffractometer producing Cu-Ka (l ¼ 1.5406 A) radiation and equipped with a solid state PIXcel detector. Mass spectrometry was performed at the Mass Spectrometry Analysis Facility at the University of Sydney on a Bruker amaZon SL mass spectrometer. Elemental microanalysis was carried out at the Chemical Analysis Facility – Element Analysis Service in the Department of Chemistry and Biomolecular Science at Macquarie University, Australia.

Electrochemistry

Solid state electrochemical measurements were performed using a BASi Epsilon Electrochemical Analyser. A three electrode set up was employed using a glassy carbon working electrode, a Pt wire counter electrode, and a Ag/Ag+ quasi-reference electrode. A 0.1 M TBAPF6/MeCN electrolyte was made and degassed with Argon prior to use. Solid samples were mechanically immobilized on the GC working electrode by grinding the electrode into a paste of the sample. Ferrocene was used as an internal standard at the end of each experiment. All values are quoted relative to the Fc/Fc+ redox couple.

UV-Vis-NIR Spectroelectrochemistry

A Cary 5000 Spectrophotometer equipped with a Harrick OmniDiff probe attachment was used to carry out UV-Vis-NIR spectroelectrochemistry. A Teflon spectroelectrochemical cell equipped with a platinum wire reference electrode, a silver wire auxiliary electrode, and an ITO coated glass cover slip as the working electrode. Solid sample was immobilized on the ITO cover slip using Teflon tape and conductive copper tape. The applied potential was controlled using eDAQ e-corder 410 potentiostat. A TBAPF6/MeCN 0.1 M electrolyte was used for all measurements. Data was reported as the Kulbelka-Munk transform, where $F(R) = (1-R^2)$ (R is the diffuse reflectance of the sample relative to the baseline).

EPR Spectroelectrochemistry

Solid state EPR-SEC data were collected on a Bruker EMXnano EPR spectrometer. For organic radicals, microwave attenuation was set to 8 dB and receiver gain was tuned to prevent signal saturation. The EPR SEC cell was constructed from a Pasteur pipette flame sealed at the thin end, filled to half-way with 0.1 M TBAPF6/MeCN electrolyte. Three electrodes connected to separate Cu wire inserts, held in place and isolated from each other with Teflon tape, were then immersed into the electrolyte, in a staggered fashion, featuring a short bare Pt counter electrode (0.125 mm) with a medium length Teflon coated Ag/Ag+ quasi-reference electrode (0.18 mm coated) and a long Teflon coated Pt working electrode (0.20 mm coated) that were stripped of their Teflon coating to expose 1 cm of the wire. The tip of the working electrode was connected to a piece of Pt gauze encasing the solid sample. EPR scans were run at various potentials controlled using an eDaq e-corder 410 potentionstat using the same methodology as for Vis-NIR SEC

Single crystal x-ray diffraction

Crystals were transferred directly from the mother liquor to a protective oil (paratone-N) before being mounted onto a 20 μm nylon loop affixed to a goniometer head. Single crystal X-ray diffraction data was collected, with assistance from Dr William Lewis, on an Agilent Technologies SuperNova diffractometer or on a Bruker diffractometer using Cu-Kα (λ = 1.5406 Å) radiation. Samples were cold-mounted over a dry ice environment and collections taken at 100 K under a stream of N_2, produced by an Oxford Cryostems 700 Plus cryostream. Data reduction, integration and absorption corrections were performed using the CrysAlisPro[1] software for the SuperNova collections and SAINT+[2] (part of the APEX2 software) for APEX II collections. Structure solutions were determined using SHELXT[3] and refined using either SHELXL[4] or OLEX.[5] Structure illustrations were produced using CrystalMaker 10.0.1.[6] Crystallographic data tables for all materials are located in the supplementary information.

Single Crystal UV-Vis Spectroscopy

Polarised single crystal UV-Vis spectroscopy was performed using a customized spectrophotometer. The apparatus was composed of optics obtained from a CARY14 spectrophotometer equipped with a 24 V/150W quartz halogen lamp and a Spec 1704, 1 m, high resolution Czerny-Turner monochromator with 500, 1000, and 1600 nm gratings and a fitted high speed stepped motor. A single crystal was mounted over a 1 mm aperture and data were collected over a 300-650 nm energy range in both horizontal and vertical polaristion modes. A baseline correction was applied to the data by measuring the absorbance spectra of the empty aperture, which was then manually subtracted from the absorption spectra of the crystal.

Molecular Orbital Calculations

Standard computational chemistry calculations were carried out with Gaussian 16.[1] Geometries were obtained from the experimental crystal structure. The stacked dimer models used in the calculations have the terminal pyridines replaced by benzenes. This is to avoid the participation of the nitrogen lone pairs in the reactions or excitations that are being investigated; presumably, such lone pairs are tied up by the coordinated Cd^{2+} cations in the actual framework environment. Electronic excitation spectra were calculated with the CAM-B3LYP[2] density functional theory method, in conjunction with the 6-31G(d)[3] basis set. We use the long-range corrected[4] CAM-B3LYP method to ensure the proper description of any prospective charge-transfer excitations. The choice of using the 6-31G(d) basis set is based on our previous studies,[5,6] which show that it provides an efficient and adequate means to account for the relative absorption

energies. The Tamm-Dancoff approximation[7] was applied to further accelerate the computation of the electronic excited states with minimal loss of accuracy.

Elemental Analysis

Prior to elemental analysis (EA) the samples were solvent exchanged in EtOH for several days.C, H, N, S analysis was carried out at the Chemical Analysis Facility – Element Analysis Service in the Department of Chemistry and Biomolecular Science at Macquarie University, Australia.

Additional Synthetic Details

General Synthetic Procedure for Py$_2$TTF containing Frameworks: Cd(NO$_3$)$_2$·4H$_2$O (11 mg, 0.036 mmol) was dissolved in ethanol (0.75 mL) by sonication. Separately, solutions of Py$_2$TTF (13.5 mg, 0.0376 mmol) in DMF (1.0 mL) and the respective coligand (0.0375 mmol) in DMF (1.5 mL) were prepared in the absence of light. Once fully solubilised the three solutions were combined into a single vial, sonicated briefly and heated at 90 °C for 48 hours in the absence of light. The following frameworks were synthesized using the above procedure.

1 (Cd(Py$_2$TTF)$_2$(bpdc)$_2$)): Cd(NO$_3$)$_2$·4H$_2$O (11 mg, 0.036 mmol) was reacted with Py$_2$TTF (13.5 mg, 0.0376 mmol) and 4,4'-biphenyldicarboxylic acid (**bpdc**) (9.10 mg, 0.0376 mmol). Framework **1** was obtained as dark-red, plate-like crystals (15.45 mg, 0.0171 mmol, 46 %). Elemental Analysis: Calculated (%) C 49.96 N 3.88 H 2.51 S 17.78. Found (%) C 50.40 N 4.12 H 3.062 S 17.028. Deviation is likely caused by the presence of 0.25 DMF and 0.5 EtOH molecules per asymmetric unit. Calculated EA values with DMF and EtOH included (%) C 50.01 N 4.13 H 3.01 S 16.81.

2 (Cd(Py$_2$TTF)$_2$(stil)$_2$)): Cd(NO$_3$)$_2$·4H$_2$O (11 mg, 0.036 mmol) was reacted with Py$_2$TTF (13.5 mg, 0.0376 mmol) and 4,4'-stilbene dicarboxylic acid (**stil**) (10.08 mg, 0.0376 mmol). Framework **2** was obtained as dark-red, plate-like crystals (11.75 mg, 0.0128 mmol, 34 %). Elemental Analysis: Calculated (%) C 51.44 N 3.74 H 2.70 S 17.16 Found (%) C 51.44 N 3.866 H 3.038 S 17.71. Deviation is likely caused by the presence of 0.25 Py$_2$TTF and 2 EtOH molecules per asymmetric unit. Calculated EA values with Py$_2$TTF and EtOH included (%) C 51.72 N 3.77 H 3.71 S 17.25.

3 (Cd(Py$_2$TTF)$_2$(oba)$_2$)): Cd(NO$_3$)$_2$·4H$_2$O (11 mg, 0.036 mmol) was reacted with Py$_2$TTF (13.5 mg, 0.0376 mmol) and 4,4'-oxybisbenzoic acid (**oba**) (9.71 mg, 0.0376 mmol). Framework **3** was obtained as dark-red, plate-like crystals (19.50 mg, 0.0211 mmol, 57 %). Elemental Analysis: Calculated (%) C: 48.88 N: 3.80 H: 2.46 S: 17.39 Found (%) C: 49.54 N: 4.94 H: 4.86 S: 15.642. Deviation is likely caused by the presence of 1 DMF and 0.5 EtOH molecules per asymmetric unit. Calculated EA values with DMF and EtOH included (%) C 49.00 N 5.04 H 3.74 S 17.25.

4 (Cd(Py$_2$TTF)$_2$(Schiff)$_2$)): Cd(NO$_3$)$_2$·4H$_2$O (11 mg, 0.036 mmol) was reacted with Py$_2$TTF (13.5 mg, 0.0376 mmol) and 4-[[(4-Carboxyphenyl)imino]methyl]benzoic acid (schiff) (9.71 mg, 0.0376 mmol). Framework **4** was obtained as dark-red, plate-like crystals (19.50 mg, 0.021 mmol, 57 %) Elemental Analysis: Calculated (%) C 49.63 N 5.60 H 2.82 S 17.09 Found (%) C 50.42 N 5.56 H 2.58 S 17.20. Deviation is likely caused by the presence of 0.25 EtOH molecules per asymmetric unit. Calculated EA values with EtOH included (%) C 49.67 N 5.51 H 2.97 S 16.83.

General Synthetic Procedures for Py₂Ph₂TTF containing frameworks: $Cd(NO_3)_2 \cdot 4H_2O$ (7.09 mg, 0.026 mmol) was dissolved in ethanol (0.75 mL) by sonication. Separately, solutions of Py₂Ph₂TTF (13.5 mg, 0.026 mmol) in DMF (2.0 mL) and the respective coligand (0.026 mmol) in DMF (1.5 mL) were prepared in the absence of light. Once fully solubilised the three solutions were combined into a single vial, sonicated briefly and heated at 90 °C for 48 hours in the absence of light. The following frameworks were synthesized using the above procedure.

1E [Cd(Py₂Ph₂TTF)₂(bpdc)₂]: $Cd(NO_3)_2 \cdot 4H_2O$ (7.09 mg, 0.026 mmol) was reacted with Py₂Ph₂TTF (13.5 mg, 0.026 mmol) and 4,4'-biphenyldicarboxylic acid (**bpdc**) (6.29 mg, 0.026 mmol). Framework **1E** was obtained as dark-red, plate-like crystals (2.96 mg, 0.00286 mmol, 11 %). Elemental Analysis: Calculated (%) C 57.76 N 3.20 H 3.00 S 14.68. Found (%) C 58.45 N 3.61 H 3.307 S 14.37.

3E [Cd(Py₂Ph₂TTF)₂(oba)₂]: $Cd(NO_3)_2 \cdot 4H_2O$ (7.09 mg, 0.026 mmol) was reacted with Py₂Ph₂TTF (13.5 mg, 0.026 mmol) and 4,4'-oxybisbenzoic acid (**oba**) (6.71 mg, 0.026 mmol). Framework **3E** was obtained as dark-red, plate-like crystals (3.459 mg, 0.00364 mmol, 14 %). Elemental Analysis: Calculated (%) C: 56.72 N: 3.15 H: 2.94 S: 14.42. Found (%) C: 56.72 N: 3.02 H: 2.93 S: 14.32.

Crystallography

Crystals were transferred directly from the mother liquor to a protective oil (paratone-N) before being mounted onto a 20 μm nylon loop affixed to a goniometer head. Single crystal X-ray diffraction data was collected, with assistance from Dr William Lewis, on an Agilent Technologies SuperNova diffractomoter or on a Bruker diffractometer using Cu-K$_\alpha$ (λ = 1.5406 Å) radiation. Samples were cold-mounted over a dry ice environment and collections taken at 100 K under a stream of N_2, produced by an Oxford Cryostems 700 Plus cryostream. Data reduction, integration and absorption corrections were performed using the CrysAlisPro[1] software for the SuperNova collections and SAINT+[2] (part of the APEX2 software) for APEX II collections. Structure solutions were determined, with assistance from Dr William Lewis and Hunter Windsor, using SHELXT[3] and refined using either SHELXL[4] or OLEX.[5] Structure illustrations were produced using CrystalMaker 10.0.1.[6]

Table S1 Crystal data and structure refinement for 1E (Deposition Number 2156708).

Identification code	dmd21_s2313_sn829_a
Empirical formula	$C_{42}H_{26}CdN_2O_4S_4$
Formula weight	863.29
Temperature/K	100(2)
Crystal system	monoclinic
Space group	C2/c
a/Å	27.8022(14)
b/Å	15.8758(5)
c/Å	29.3186(14)
α/°	90
β/°	115.368(6)
γ/°	90
Volume/Å^3	11692.9(10)
Z	8
ρ_{calc}g/cm^3	0.981
μ/mm^{-1}	4.566
F(000)	3488.0
Crystal size/mm^3	0.176 × 0.1 × 0.031
Radiation	Cu Kα (λ = 1.54184)
2Θ range for data collection/°	7.038 to 145.406
Index ranges	$-34 \leq h \leq 32, -19 \leq k \leq 17, -24 \leq l \leq 36$
Reflections collected	28889
Independent reflections	11333 [R_{int} = 0.1193, R_{sigma} = 0.1215]
Data/restraints/parameters	11333/12/448
Goodness-of-fit on F^2	1.068
Final R indexes [I>=2σ (I)]	R_1 = 0.0843, wR_2 = 0.2396
Final R indexes [all data]	R_1 = 0.1301, wR_2 = 0.2826
Largest diff. peak/hole / e Å^{-3}	2.33/-1.30

Table S2 Crystal data and structure refinement for 3 (Deposition Number 2155075).

Identification code	dmd20_s2180_fr140
Empirical formula	$C_{60}H_{36}Cd_2N_4O_{10}S_8$
Formula weight	1454.21
Temperature/K	100.0
Crystal system	triclinic
Space group	P-1
a/Å	9.4350(6)
b/Å	14.9179(10)
c/Å	15.3694(10)
α/°	117.853(2)
β/°	92.999(2)
γ/°	102.297(2)
Volume/Å^3	1839.7(2)
Z	1
ρ_{calc}g/cm^3	1.313
μ/mm^{-1}	0.855
F(000)	728.0
Crystal size/mm^3	0.1 × 0.1 × 0.01
Radiation	MoKα (λ = 0.71073)
2Θ range for data collection/°	3.044 to 56.562
Index ranges	-12 ≤ h ≤ 12, -19 ≤ k ≤ 17, -16 ≤ l ≤ 20
Reflections collected	37928
Independent reflections	9013 [R_{int} = 0.0524, R_{sigma} = 0.0576]
Data/restraints/parameters	9013/0/384
Goodness-of-fit on F^2	1.054
Final R indexes [I>=2σ (I)]	R_1 = 0.0498, wR_2 = 0.1151
Final R indexes [all data]	R_1 = 0.0759, wR_2 = 0.1262
Largest diff. peak/hole / e Å^{-3}	3.25/-0.85

Table S3 Crystal data and structure refinement for 3E (deposition number 2156707).

Identification code	dmd19ek2_s1900_a
Empirical formula	$C_{23.5}H_{19.5}Cd_{0.5}N_{1.5}O_{3.5}S_2$
Formula weight	499.22
Temperature/K	100.00(10)
Crystal system	triclinic
Space group	P-1
a/Å	9.6565(3)
b/Å	15.1597(4)
c/Å	18.3062(6)
α/°	104.990(3)
β/°	91.644(3)
γ/°	90.050(2)
Volume/Å^3	2587.47(15)
Z	4
ρ_{calc}g/cm^3	1.282
μ/mm^{-1}	5.278
F(000)	1020.0
Crystal size/mm^3	0.169 × 0.082 × 0.03
Radiation	CuKα (λ = 1.54184)
2Θ range for data collection/°	8.782 to 146.414
Index ranges	-11 ≤ h ≤ 11, -18 ≤ k ≤ 18, -22 ≤ l ≤ 22
Reflections collected	40682
Independent reflections	10096 [R_{int} = 0.0627, R_{sigma} = 0.0510]
Data/restraints/parameters	10096/4/487
Goodness-of-fit on F^2	1.039
Final R indexes [I>=2σ (I)]	R_1 = 0.0883, wR_2 = 0.2638
Final R indexes [all data]	R_1 = 0.1071, wR_2 = 0.2862
Largest diff. peak/hole / e Å^{-3}	2.55/-1.40

Table S4 Crystal data and structure refinement for 4 (deposition number 2235495).

Identification code	schiff_Py2TTF_Cd_2_a
Empirical formula	$C_{25.5}H_{25.5}N_{25.5}O_{25.5}S_{25.5}Cd_{25.5}$
Formula weight	4780.94
Temperature/K	100.0
Crystal system	monoclinic
Space group	P2/c
a/Å	21.088(4)
b/Å	16.683(3)
c/Å	32.878(7)
α/°	90
β/°	101.07(3)
γ/°	90
Volume/Å^3	11352(4)
Z	4
ρ_{calc}g/cm^3	2.797
μ/mm^{-1}	5.190
F(000)	8772.0
Crystal size/mm^3	? × ? × ?
Radiation	MoKα (λ = 0.71073)
2Θ range for data collection/°	1.968 to 63.962
Index ranges	-28 ≤ h ≤ 28, -23 ≤ k ≤ 23, -42 ≤ l ≤ 42
Reflections collected	199426
Independent reflections	32326 [R_{int} = 0.1464, R_{sigma} = 0.0900]
Data/restraints/parameters	32326/1159/1134
Goodness-of-fit on F^2	0.911
Final R indexes [I>=2σ (I)]	R_1 = 0.0998, wR_2 = 0.3003
Final R indexes [all data]	R_1 = 0.2209, wR_2 = 0.3979
Largest diff. peak/hole / e Å^{-3}	1.55/-0.84

Table S5: Number of electrons removed using the SQUEEZE mask as well as their likely identities.

Framework	e$^-$ removed using SQUEEZE	Likely identity
1E	121	3.6 × DMF or 2 × DMF and 2 × EtOH
2	30	1 × DMF
3	72	2 × DMF or 1 × DMF and 1.5 × EtOH
3E	None, 1 EtOH and 1 DMF were modelled	
4	200	6 × DMF or 1.5 × Py$_2$TTF in pore

Table S6: 1st Oxidation potential for various frameworks.

FRAMEWORK	1ST OXIDATION POTENTIAL (V)
1-BPDC	0.108
1E-BPDC	0.072
2-STILL	0.164

3-OBA	0.207
3E-OBA	0.035
4-SCHIFF	0.092
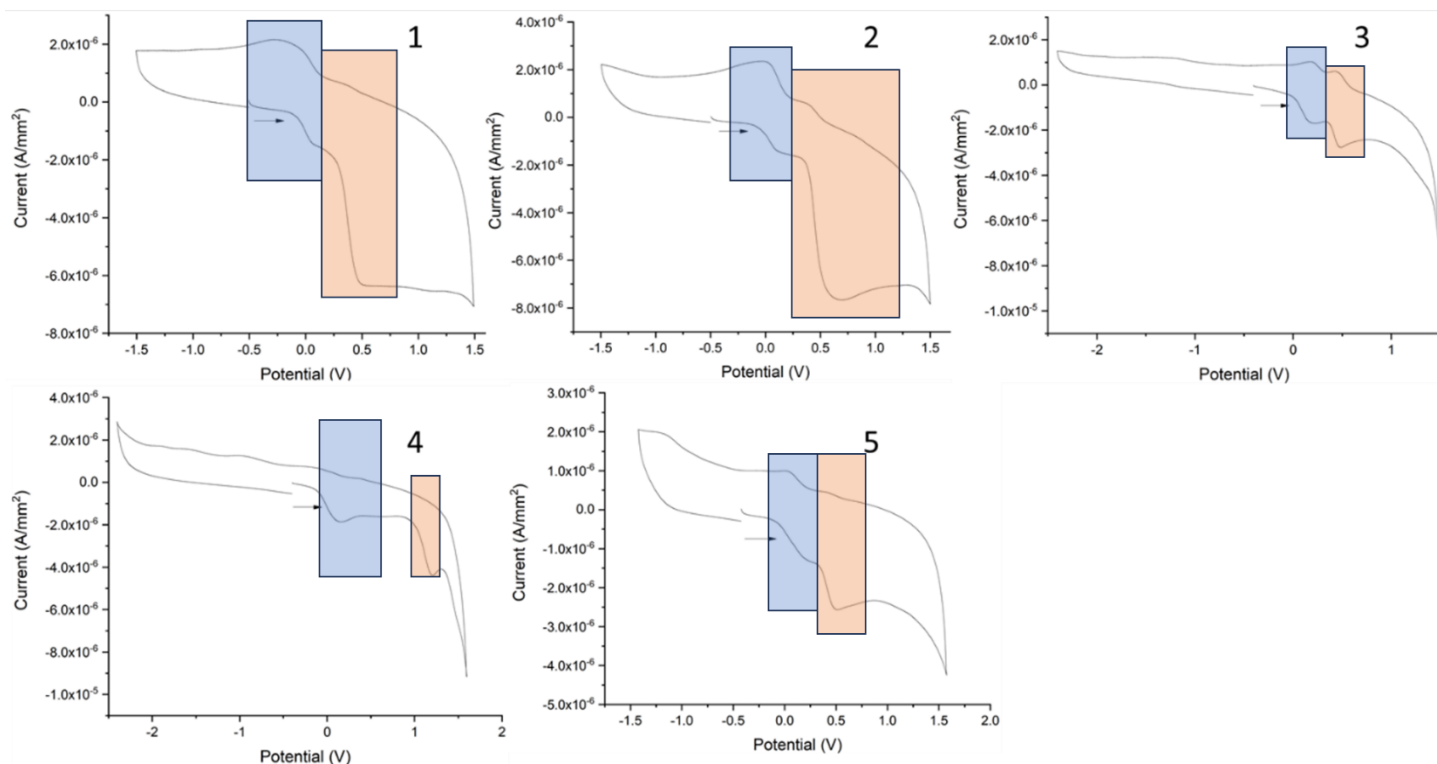
Figure S1: 200 mVs⁻¹Cyclic Voltammograms of 1. [Cd(stil)₂(Py₂TTF)₂] 2.[Cd(Schiff)₂(Py₂TTF)₂], 3.[Cd(oba)₂(Py₂TTF)₂], 4. [Cd(oba)₂(Py₂Ph₂TTF)₂], 5. [Cd(bpdc)₂(Py₂Ph₂TTF)₂. The first 1 electron oxidation is highlighted in blue and the second 1 electron oxidation is highlighted in blue.
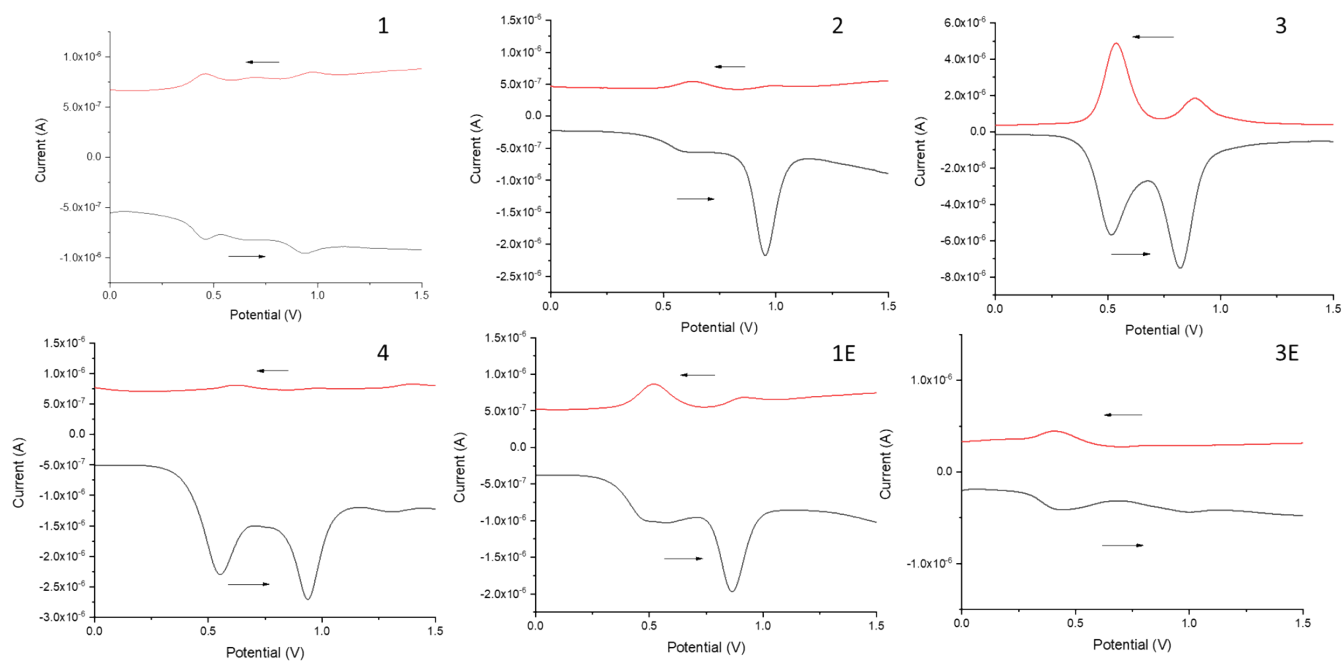
Figure 2: Square wave voltammograms for the frameworks reported in this paper.
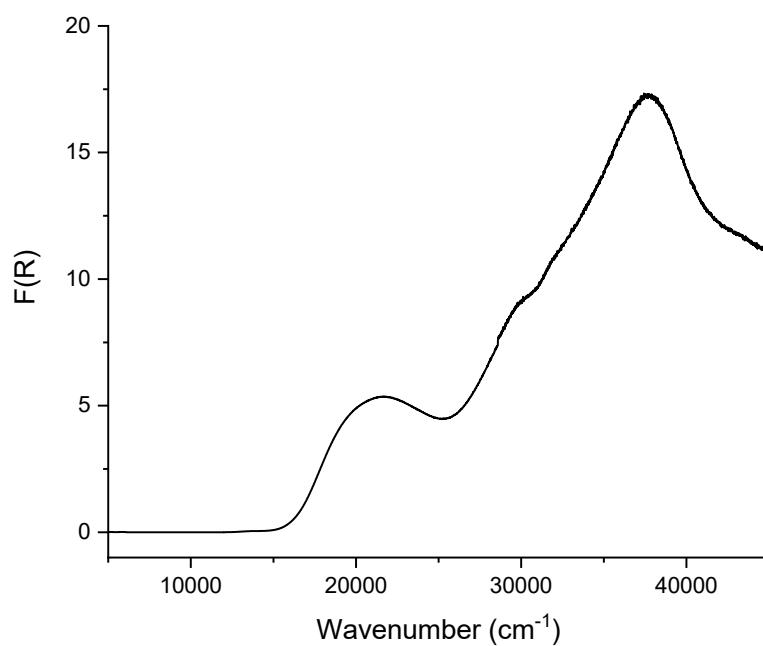
Figure S3: Solid-state UV-Vis Spectrum of 1E
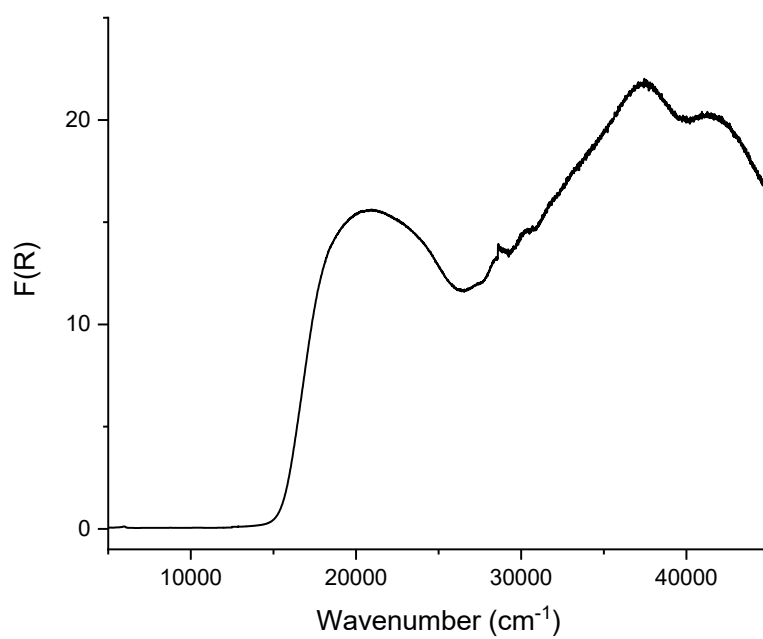
Figure S4: Solid-state UV-Vis spectrum of 2
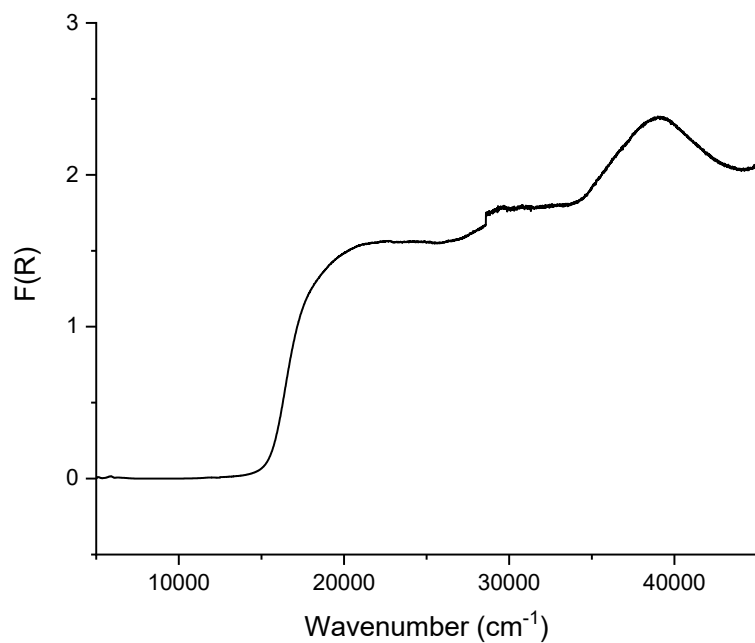
Figure S5: Solid-state neutral UV-Vis spectrum of 3
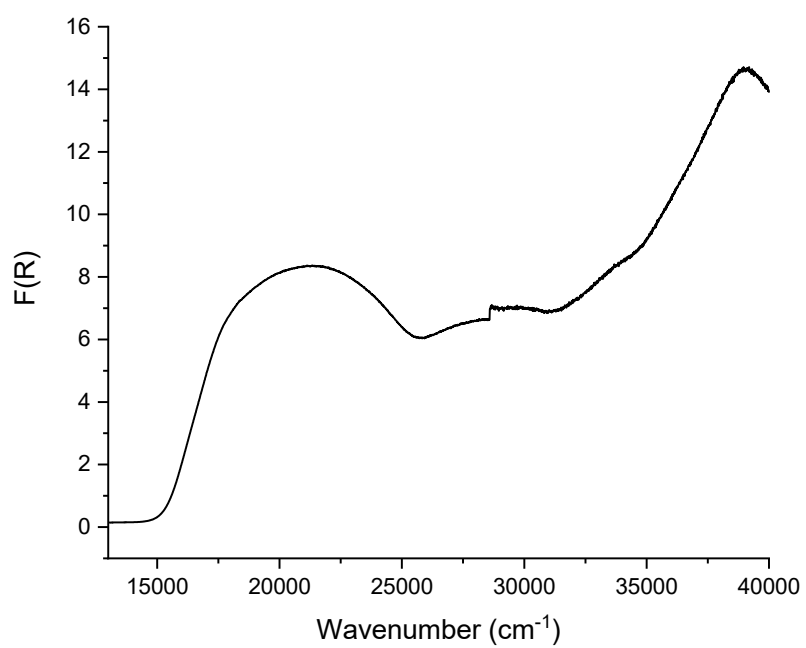
Figure S6: Solid-State UV-Vis Spectrum of 3E
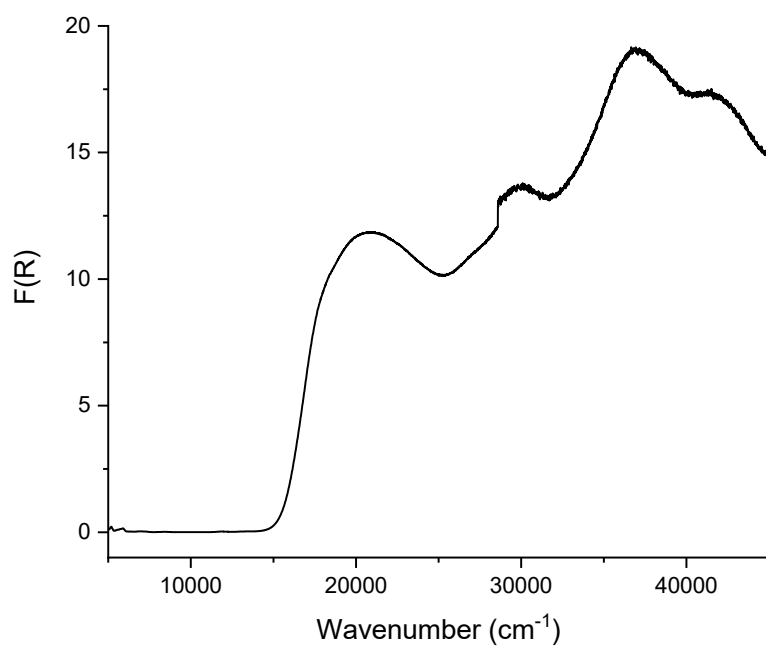
Figure S7: Solid-state neutral UV-Vis spectrum of 4
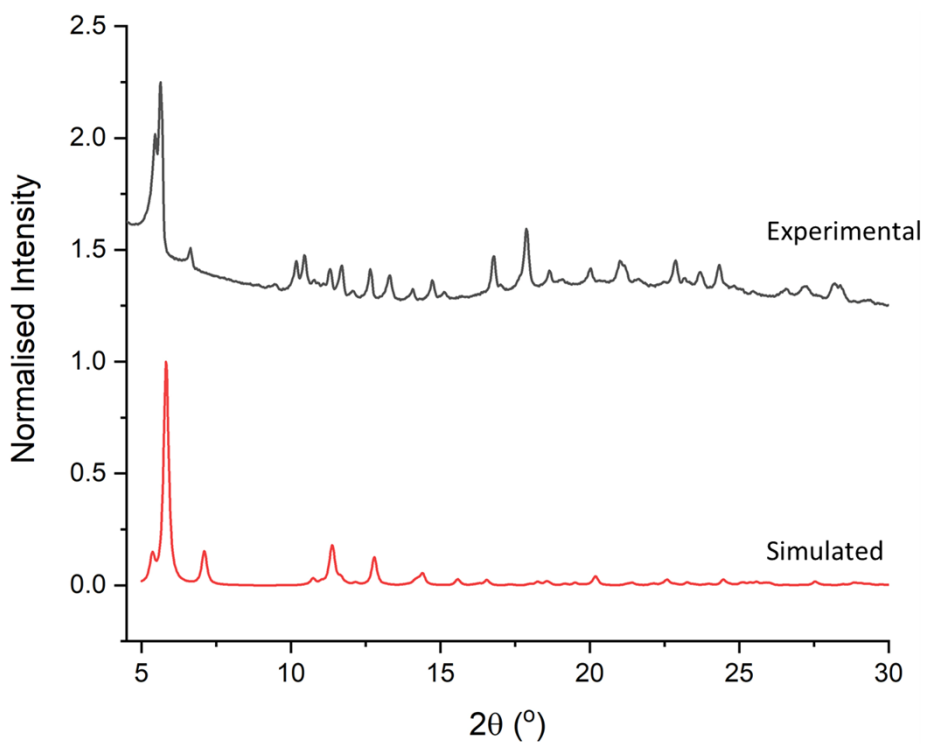
Figure S8: PXRD pattern of 2 simulated (red) and experimental (black)
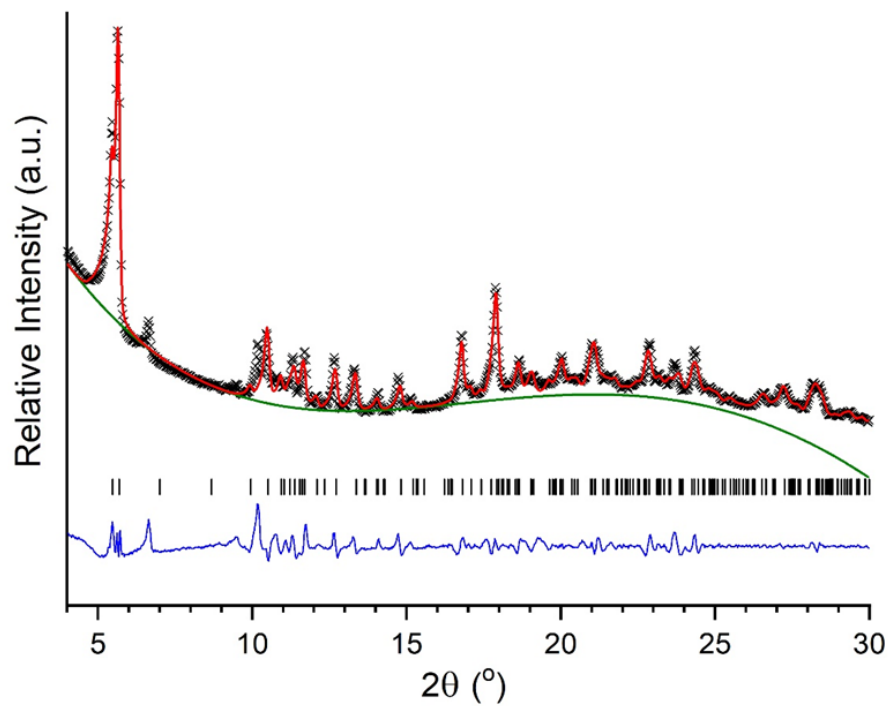
Figure S9: Le Bail refinement of 2. Refinement converged at an Rwp of 4.512.
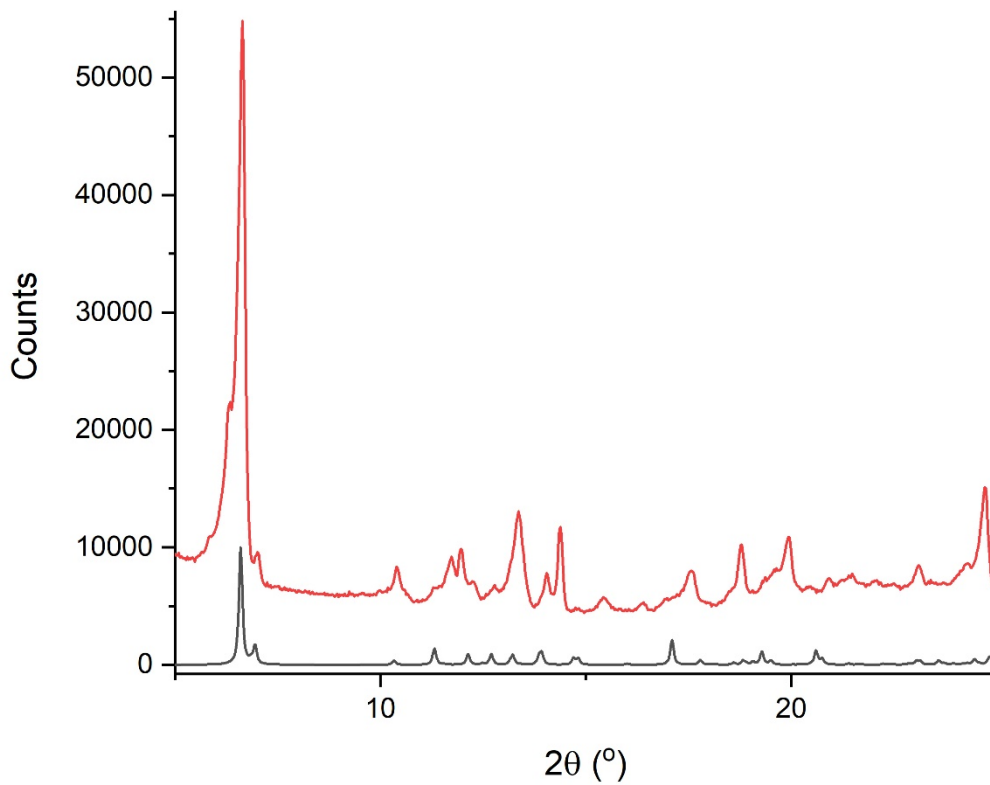
Figure S10: PXRD pattern of 3 simulated (black) and experimental (red).
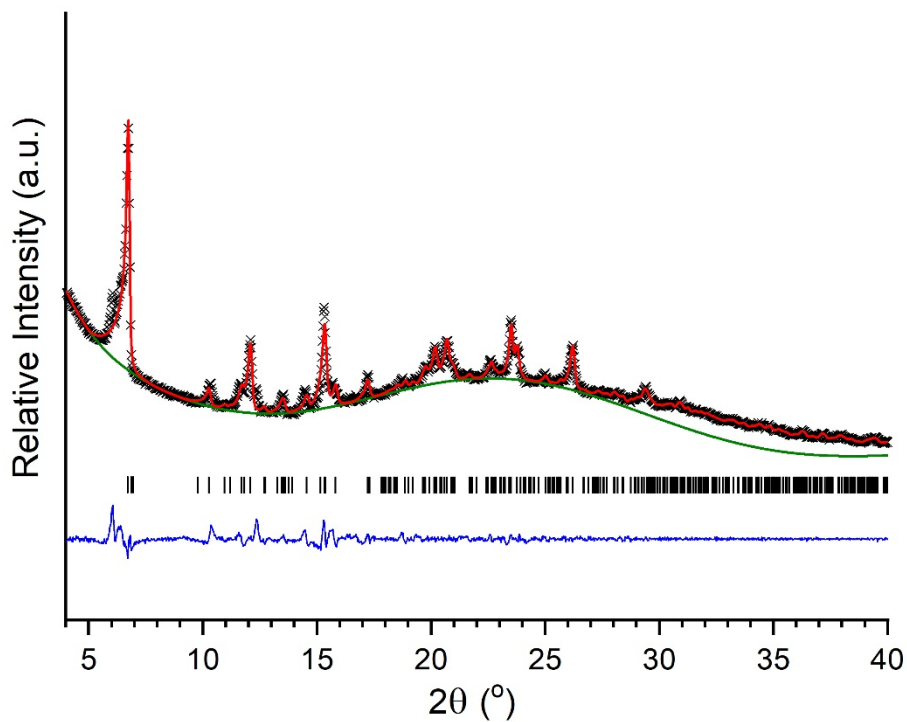
Figure S11: Le Bail refinement of 3. Refinement converged with an Rwp = 3.209
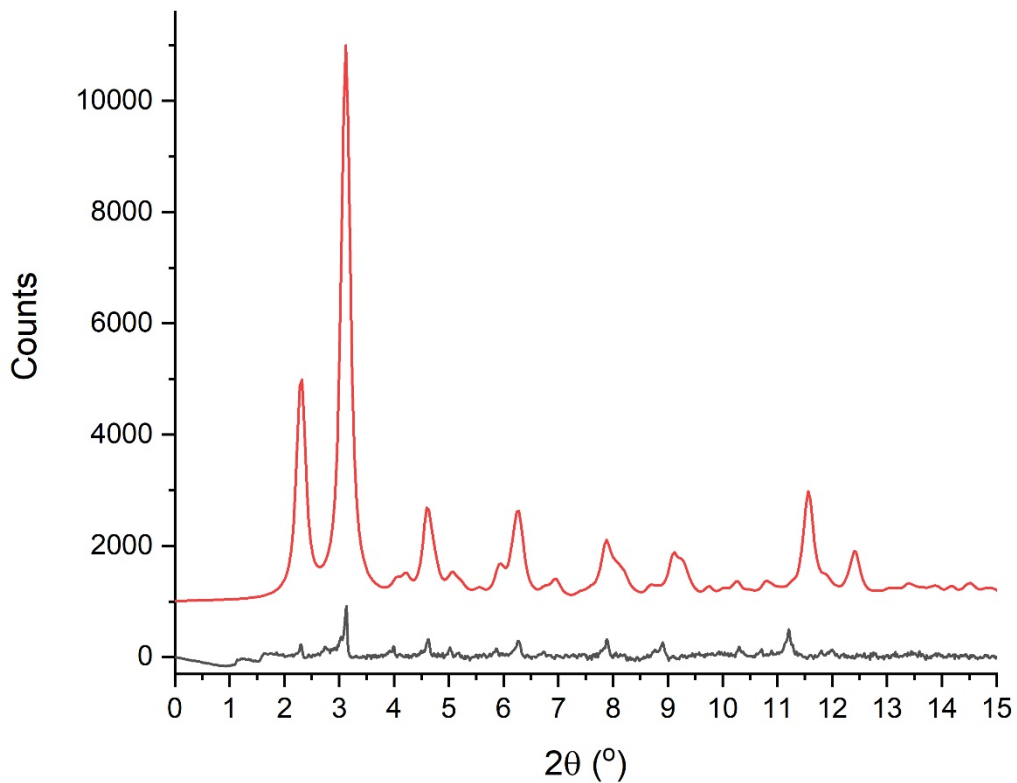
Figure S12:PXRD pattern of 3E simulated (black) and experimental (red). Collected on a STOE capillary XRD fitted with a Mo source.
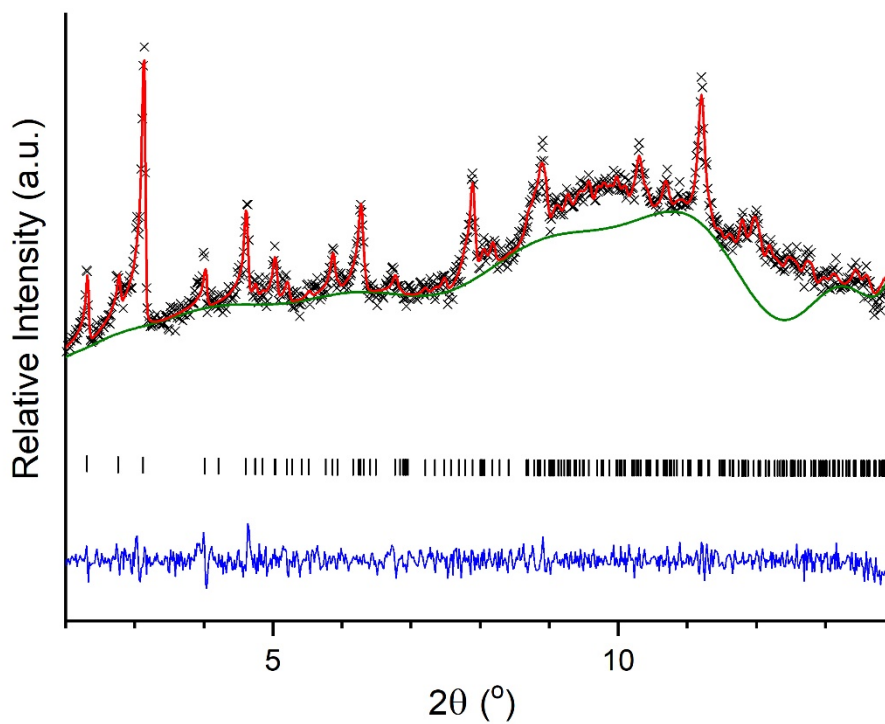
Figure S13: Le Bail refinement of 3E. Refinement converged with an Rwp = 3.969
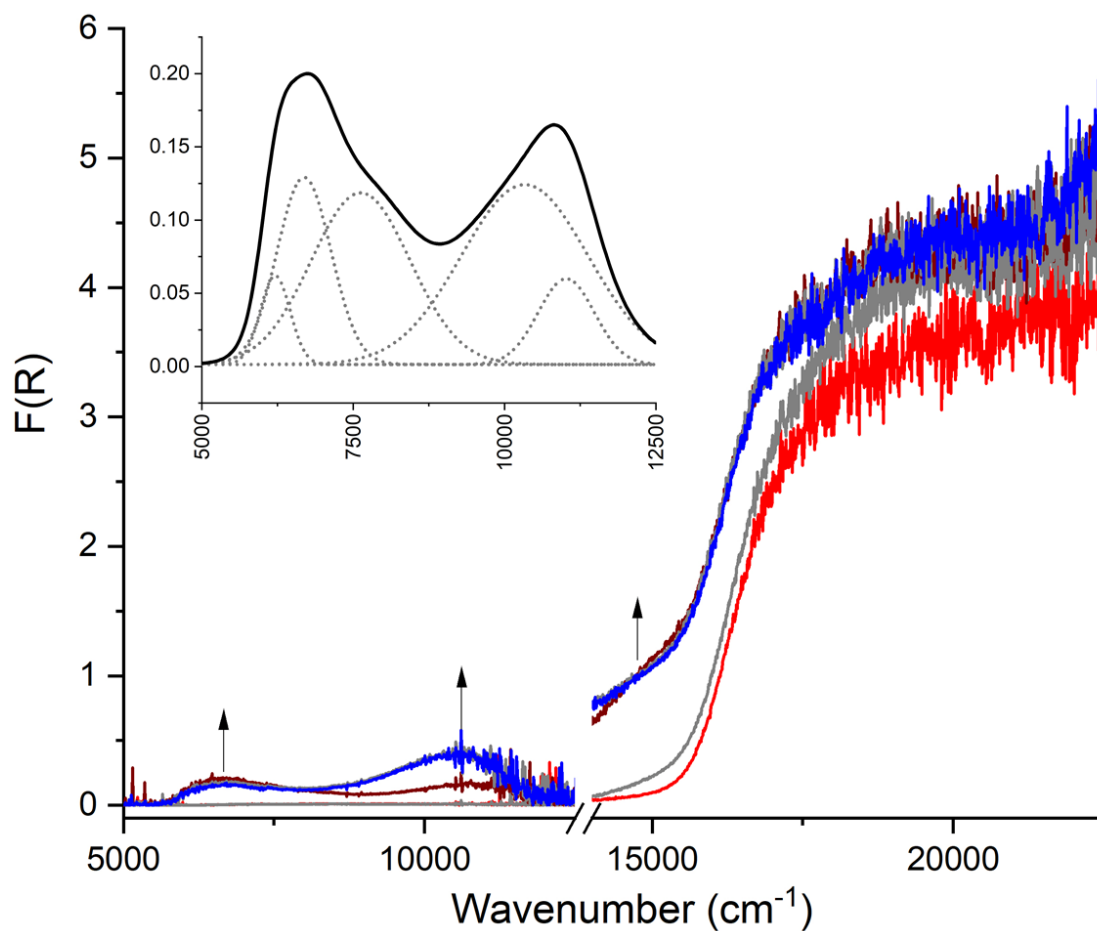
Figure S14: Spectral progression of [Cd(stil)$_2$(Py$_2$TTF)$_2$] from 0-1.7 V. Detector change between 12500 and 14000 cm^{-1} has been removed. 0.0 V spectrum is shown in red, 1.7 V spectrum is shown in blue, and 1.3 V spectrum where IVCT is maximised is shown in burgundy. Inset shows deconvolution of NIR region at 1.3 V.
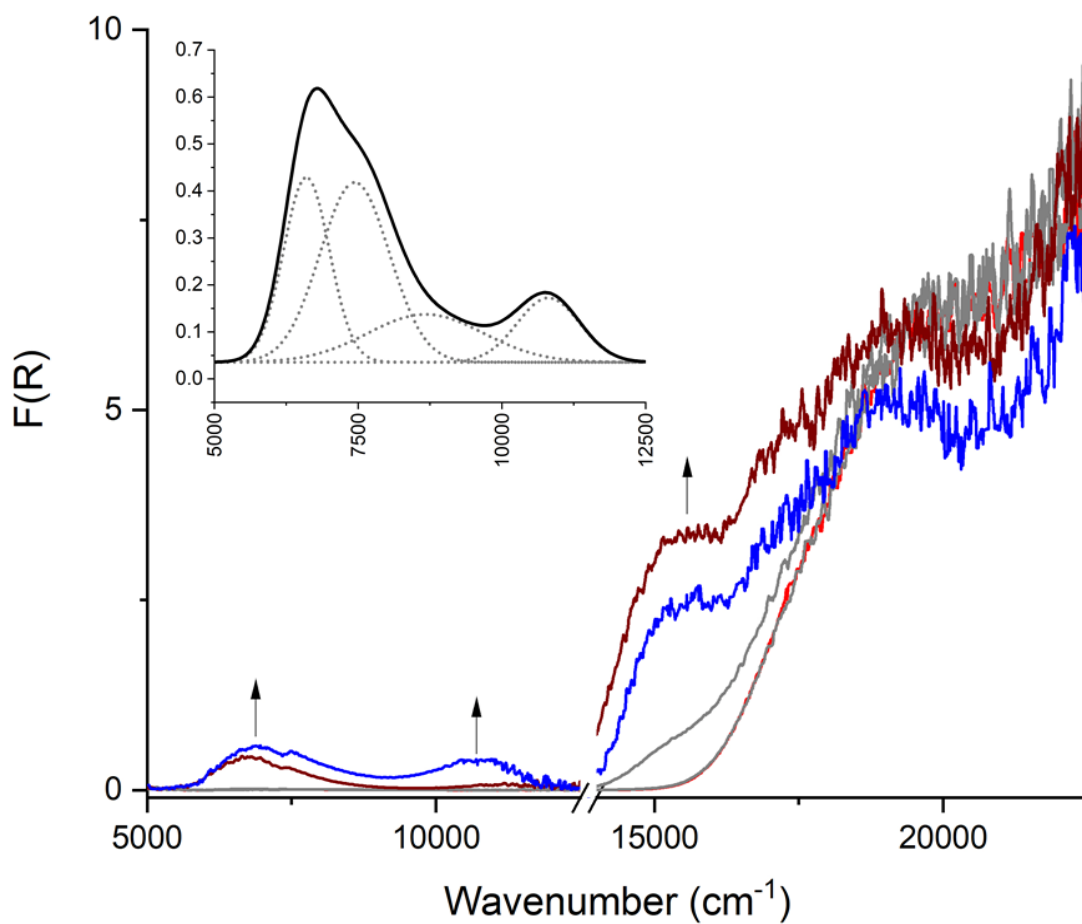
Figure S15: Spectral progression of [Cd(schiff)$_2$(Py2TTF)$_2$] from 0-1.8 V. Detector change between 12500 and 14000 cm-1 has been removed. 0.0 V spectrum is shown in red, 1.7 V spectrum is shown in blue, and 1.3 V spectrum where IVCT is maximised is shown in burgundy. Inset shows deconvolution of NIR region at 1.3 V.
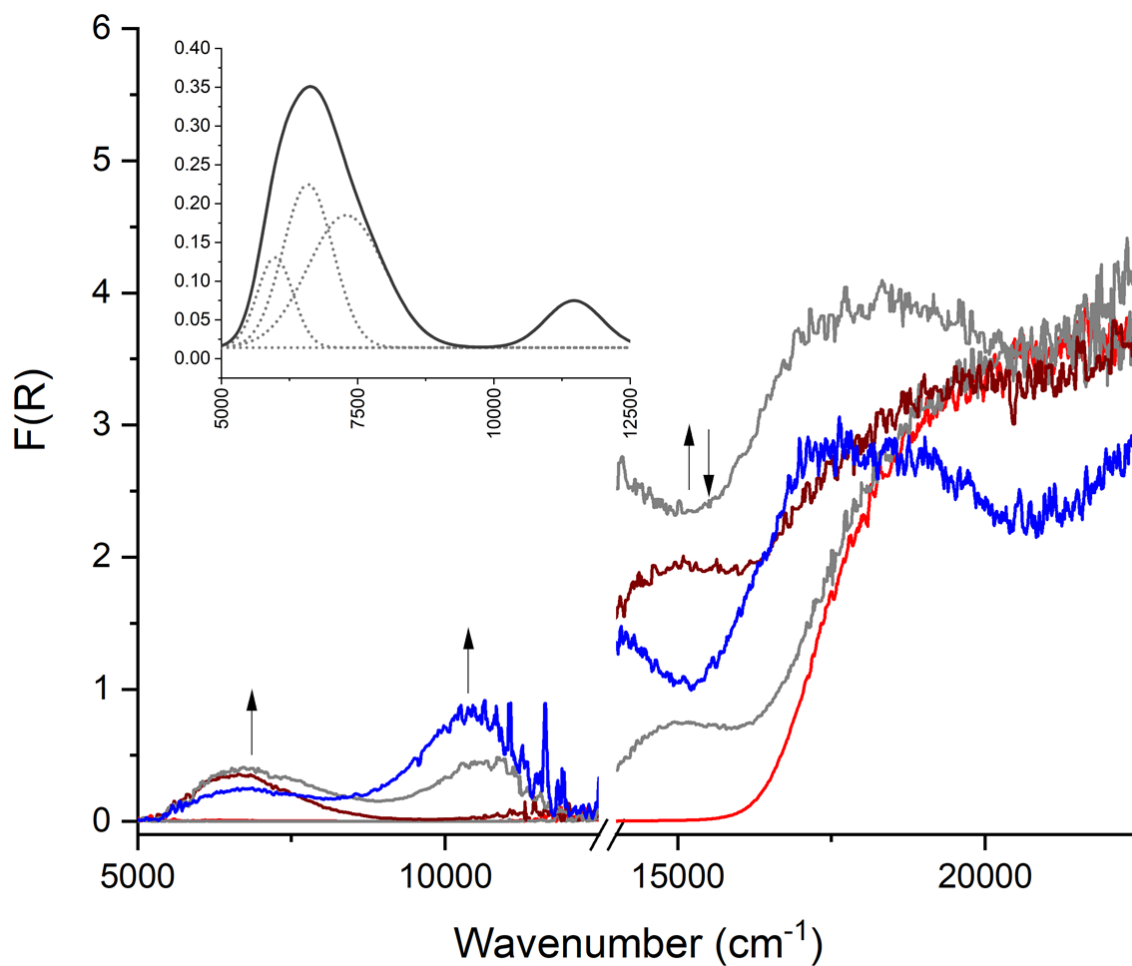
Figure S16: Spectral progression of [Cd(oba)₂(Py₂TTF)₂] from 0.0 – 2.0 V. Detector change between 12500 and 14000 cm-1 has been removed. 0.0 V spectrum is shown in red, 2.0 V spectrum is shown in blue, and 1.0 V spectrum where IVCT is maximised is shown in burgundy. Inset shows deconvolution of NIR region at 1.0 V.
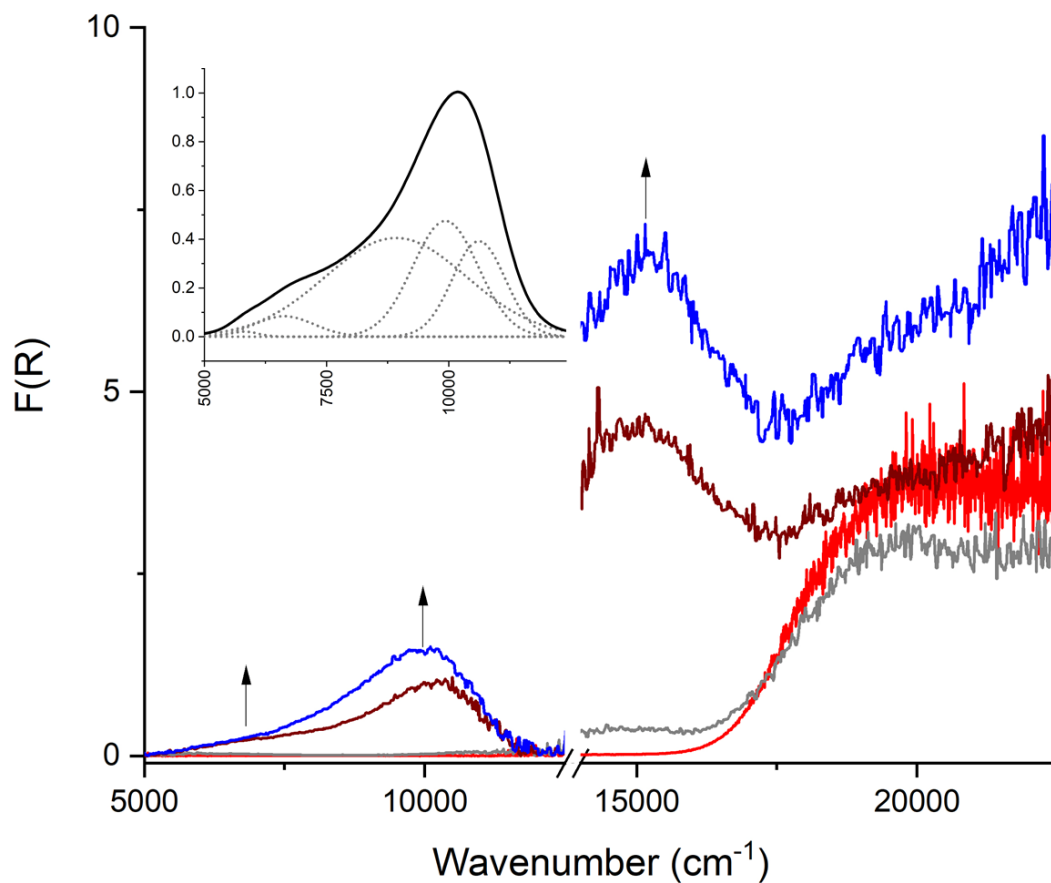
Figure S17: Spectral progression of [Cd(oba)₂(Py₂Ph₂TTF)₂] from 0.0 – 2.0 V. Detector change between 12500 and 14000 cm-1 has been removed. 0.0 V spectrum is shown in red, 2.0 V spectrum is shown in blue, and 1.3 V spectrum where IVCT is maximised is shown in burgundy. Inset shows deconvolution of NIR region at 1.3 V.
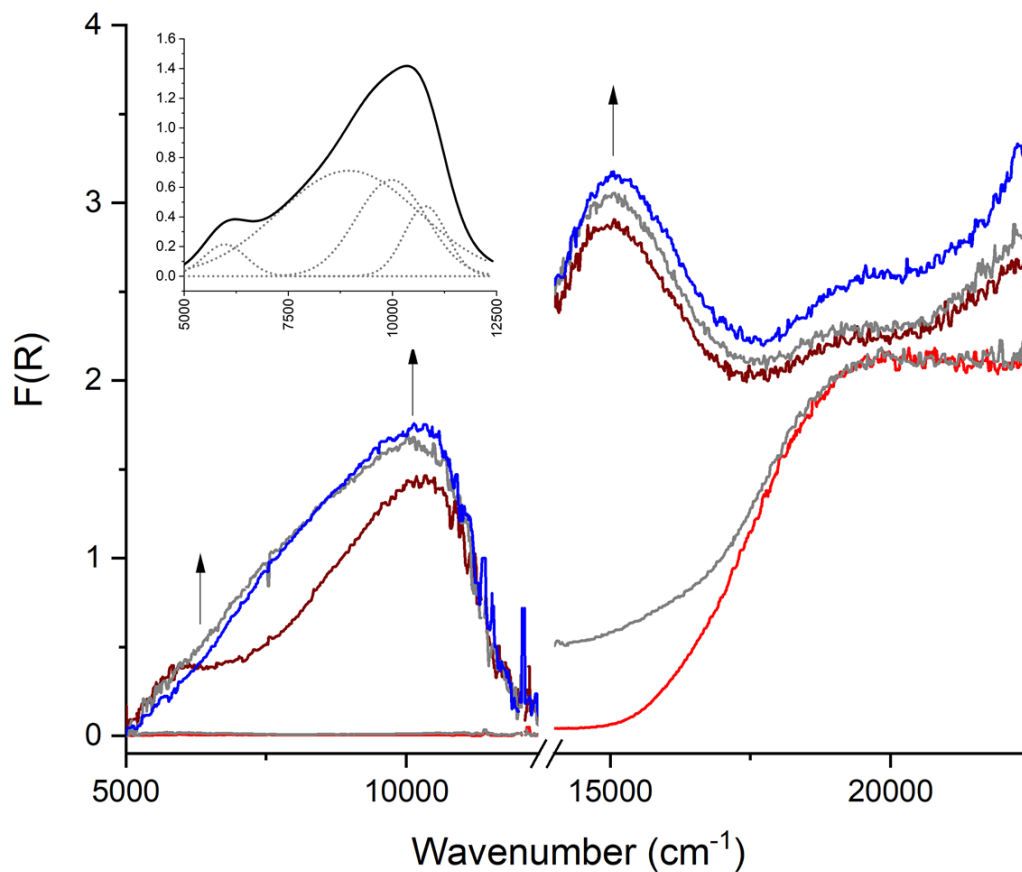
Figure S18:Spectral progression of [Cd(bpdc)2(Py2Ph2TTF)2] from 0.0 – 2.0 V. Detector change between 12500 and 14000 cm-1 has been removed. 0.0 V spectrum is shown in red, 2.0 V spectrum is shown in blue, and 1.3 V spectrum where IVCT is maximised is shown in burgundy. Inset shows deconvolution of NIR region at 1.3 V.
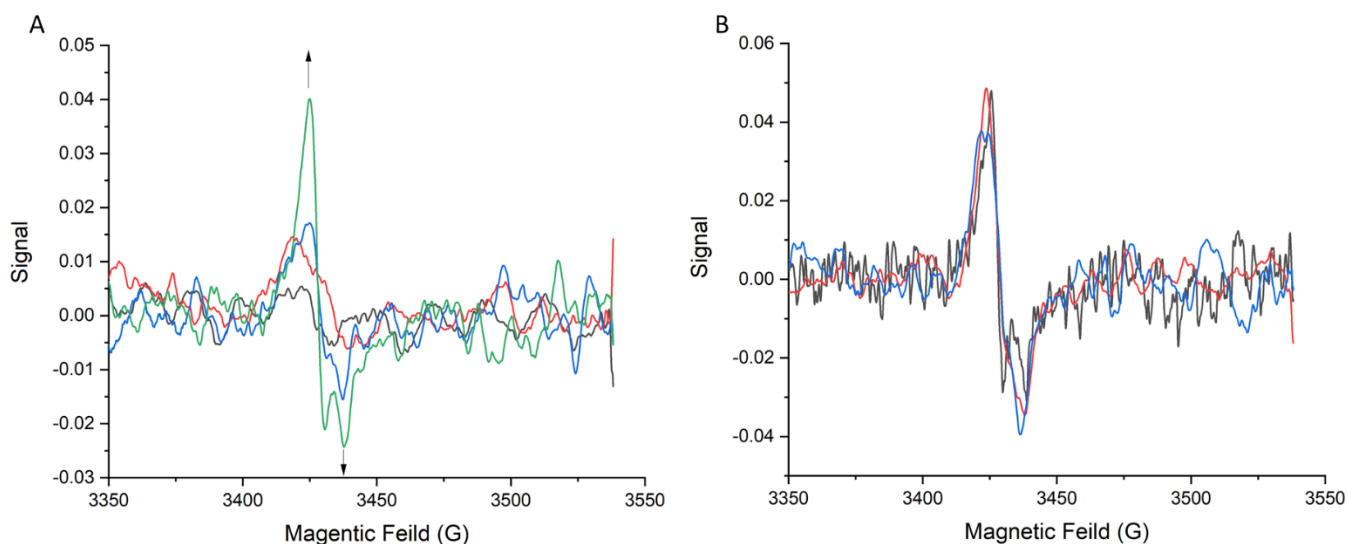
Figure S19: SEC-EPR spectrum of 1E. Displayed at 0.5 V intervals A) from 0.0 V – 2.0 V. B) from 2.0 V – 0.0 V.
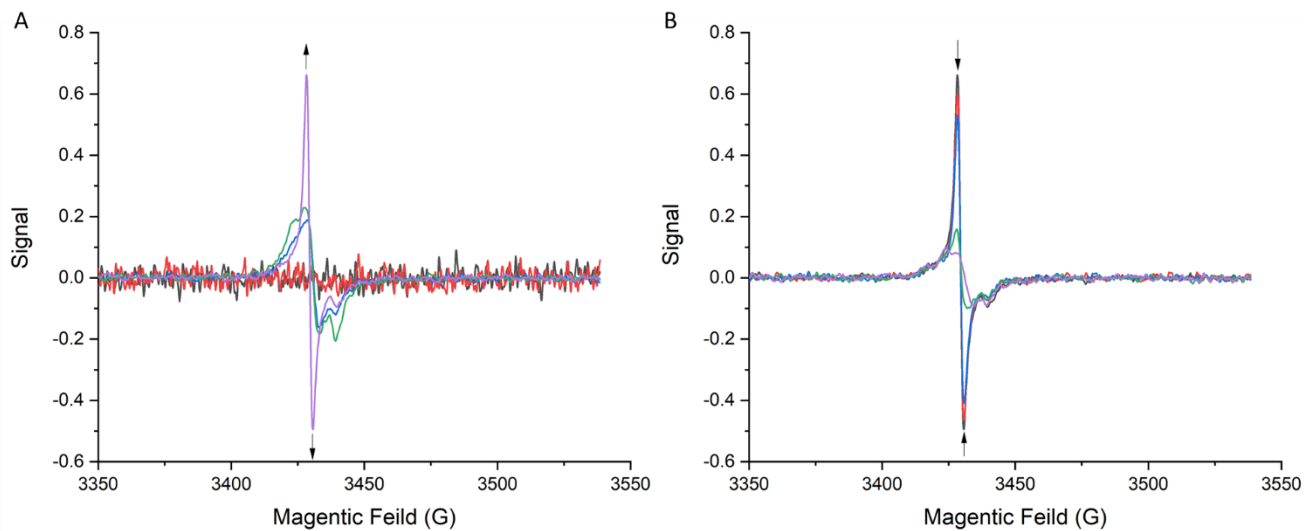
Figure S20: SEC-EPR spectrum of 2. Displayed at 0.5 V intervals A) from 0.0 V – 2.0 V. B) from 2.0 V – 0.0 V.
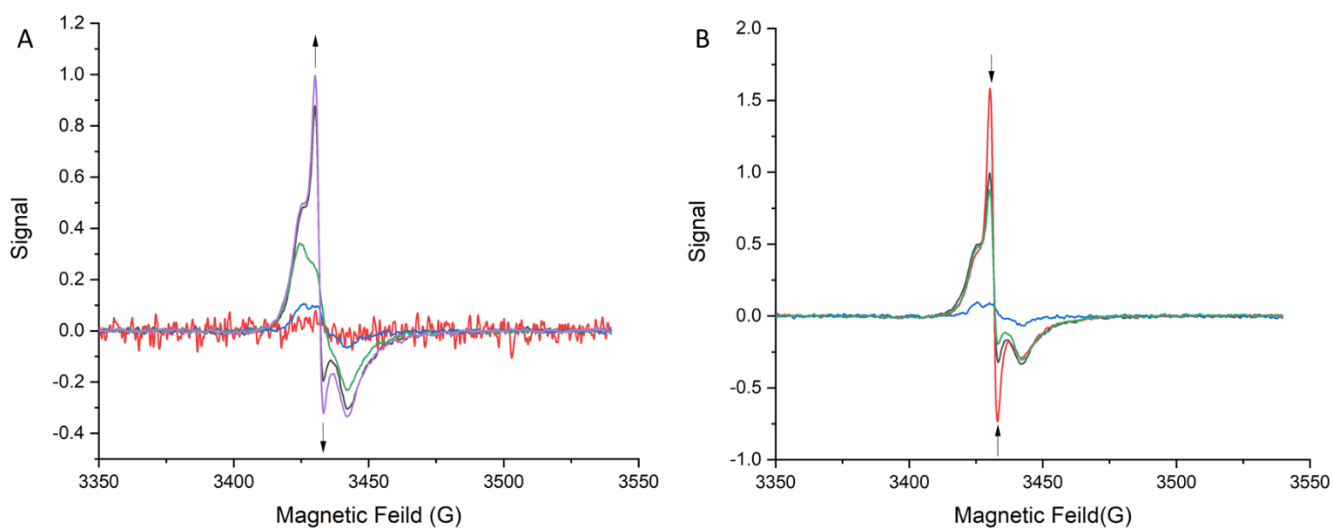
Figure S21: SEC-EPR spectrum of 3. Displayed at 0.5 V intervals A) from 0.0 V - 2.0 V B) from 2.0 V - 0.0 V.
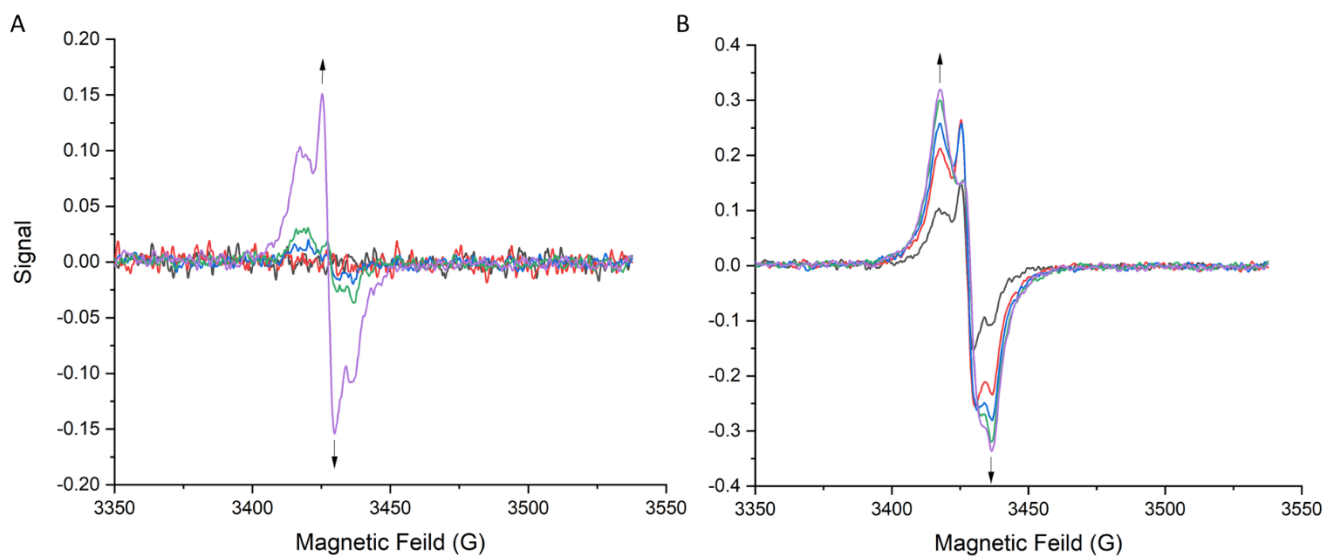
Figure S22: SEC-EPR spectrum of 3E. Displayed at 0.5 V intervals A) from 0.0 V - 2.0 V B) from 2.0 V - 0.0 V.
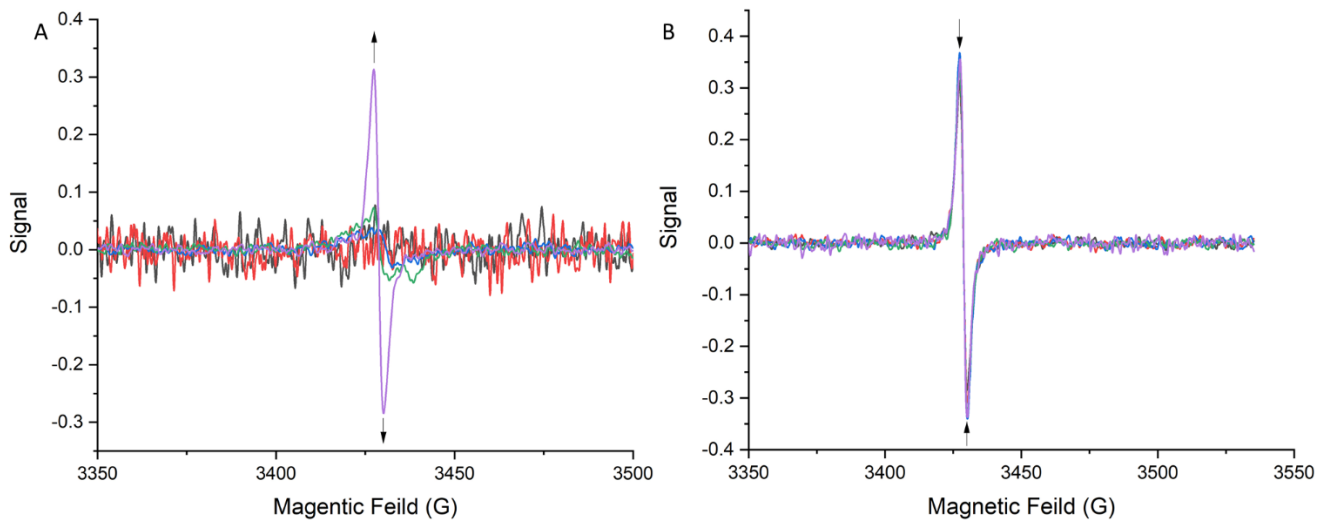
Figure S23: SEC-EPR spectrum of 4. Displayed at intervals of 0.5 V A) from 0.0 V - 2.0 V. B) from 2.0 V – 0.0 V
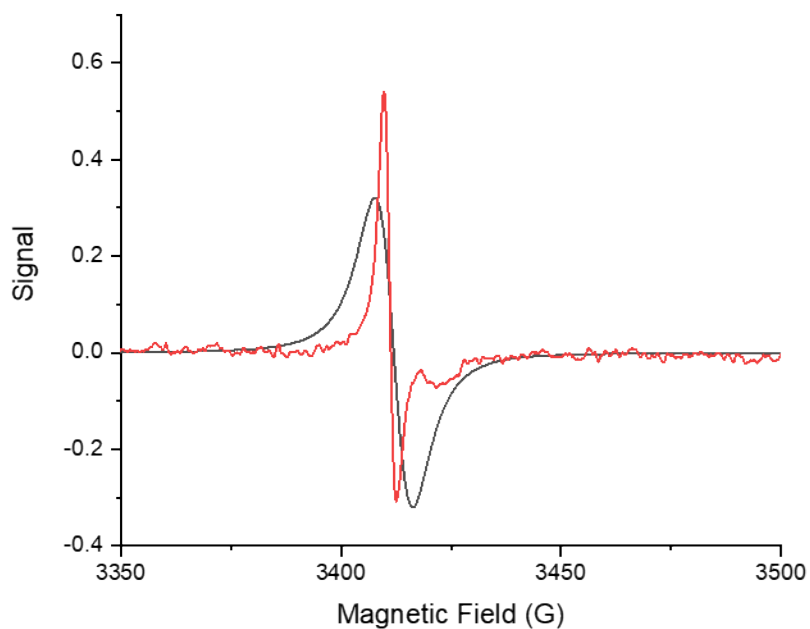
Figure S24: Easyspin fitting of Framework 1. RMSD: 0.0894. g_x, g_y, g_z: 2.0136, 2.0136, 2.00136. Raw data is shown in red, easyspin simulation is shown in black.
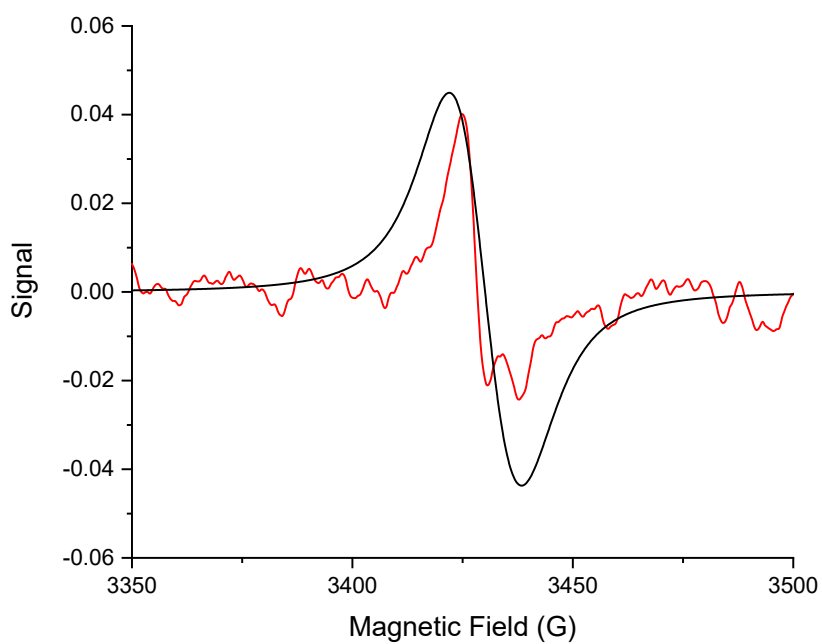
Figure S25: Easyspin fitting of Framework 1E. RMSD: 8.7830. g_x, g_y, g_z: 2.0098, 2.0125, 2.0125. Raw data is shown in red, easyspin simulation is shown in red.
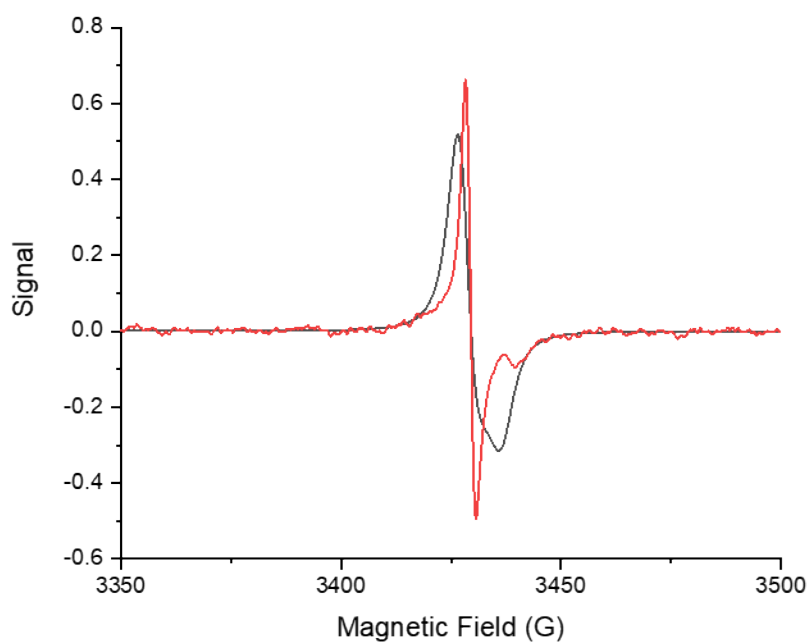

Figure S26: Easyspin fitting of Framework 2. RMSD: 1.3535. g_x, g_y, g_z: 2.0154, 2.0206, 2.0206. Raw data is shown in red, easyspin simulation is shown in black.
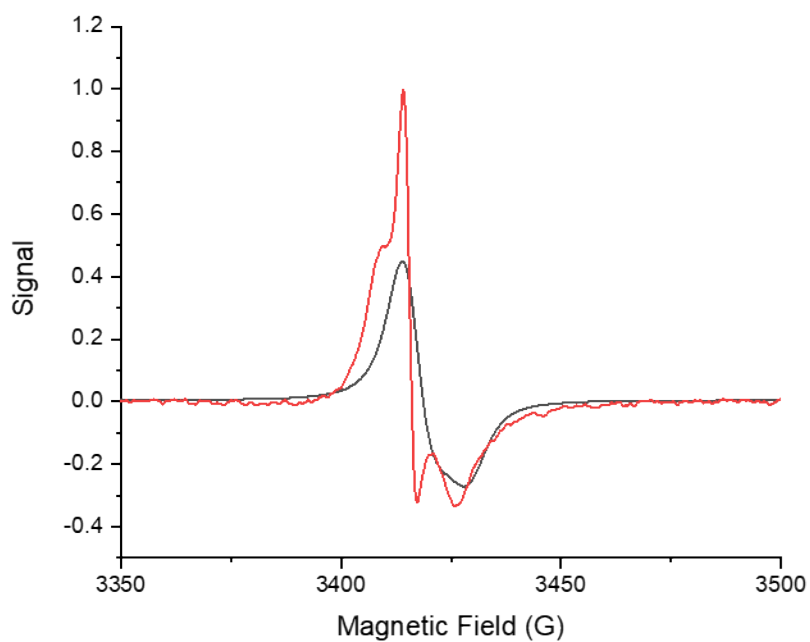
Figure S27: Easyspin fitting of Framework 3. RMSD: 2.8385. g_x, g_y, g_z: 2.0210, 2.0210, 2.0131. Raw data is shown in red, easyspin simulation is shown in black.
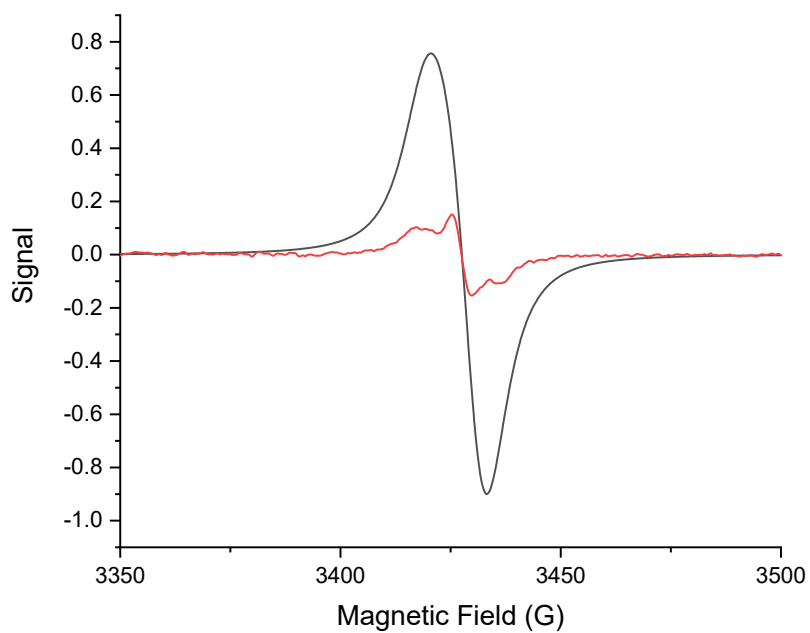

Figure S28: Easyspin fitting of Framework 3E. RMSD: 3.1209. g_x, g_y, g_z: 2.0211, 2.0247, 2.0218. Raw data is shown in red, easyspin simulation is shown in black.
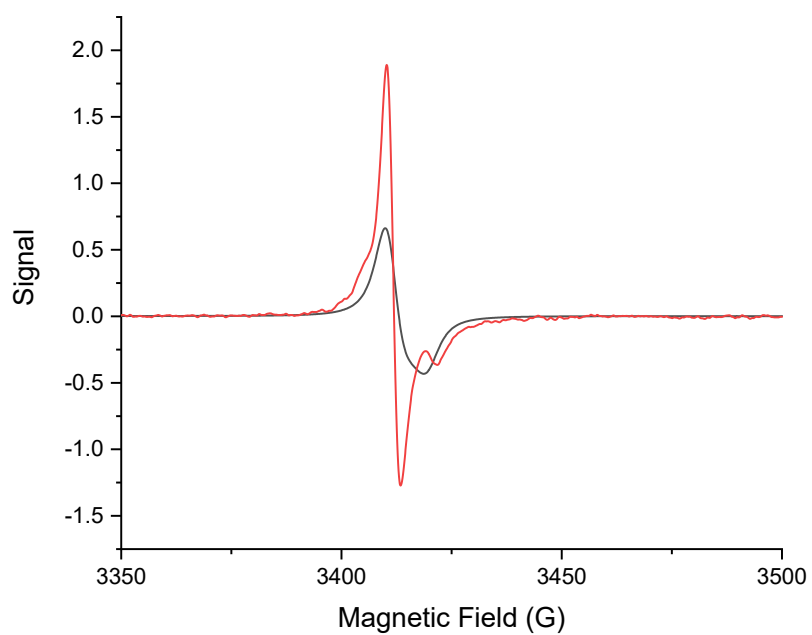
Figure S29: Easyspin fitting of Framework 4. RMSD: 1.6309. g_x, g_y, g_z: 2.0250, 2.0250, 2.0201. Raw data is shown in red, easyspin simulation is shown in black.

Images for crystal measurements

Crystal width was determined by taking an image of the crystal used in the single crystal UV-Vis adsorption experiment propped on its side. Three measurements were taken across the width of the crystal using the Fiji image software. The ratio of pixels across the crystal to pixels in the scale bar was used to determine the width of the crystal.
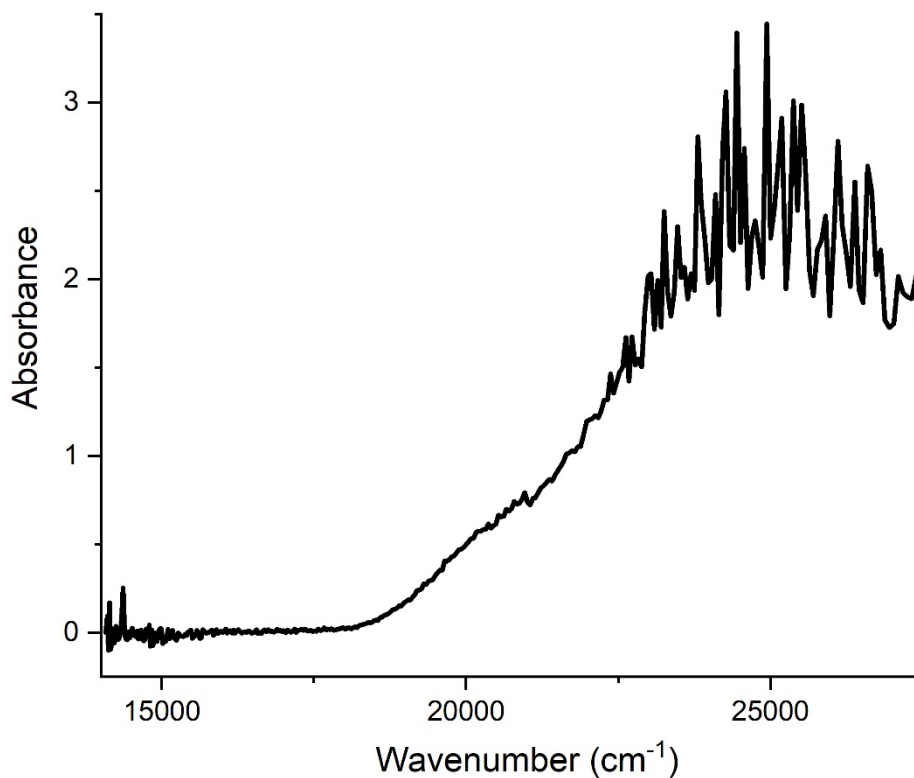

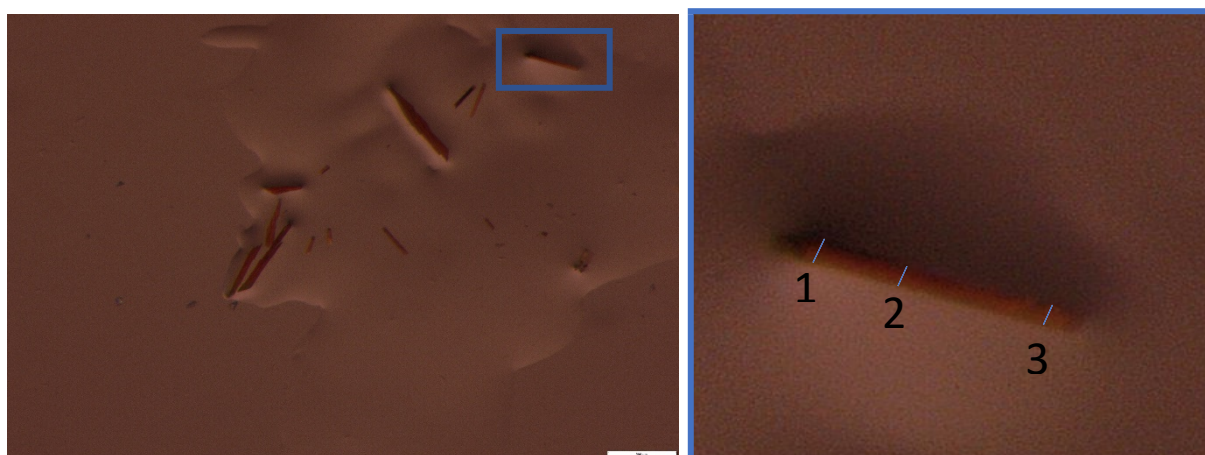**Figure S30: SC-UV-Vis spectrum of 1 from horizontally polarised light**

Figure S31: Crystal images of 1 used to measure the width of the crystal

Calculation of Crystal width

1: 18.514 pixels 2: 14.886 pixels 3: 17.088 pixels Av width = 16.829 pixels

200 μm Scale bar: 255 pixels therefore 0.784 μm/pixel

Width of crystal = 0.784 x 16.829 = 13.199 μm = 0.013199 mm = 0.0013199 cm

Table S7: Spectral data for 1

v_{max} (cm⁻¹)*	F(R)$_{max}$ (a.u.)	$\Delta v_{1/2}$ (cm⁻¹)	$\Delta v_{1/2}°$ (cm⁻¹)	ε (M⁻¹ cm⁻¹)	H$_{ab}$ (cm⁻¹)
6479(178)	0.33(9)	1221(165)	3935	91(34)	145(40)
7775	0.171	1113	4238		
9981	0.190	5009	4802		
10669	0.300	1111	4964		
14991	0.557	1533	5885		
17471	1.496	3153	6353		
19524	0.823	1922	6716		
23262	2.614	6127	7330		

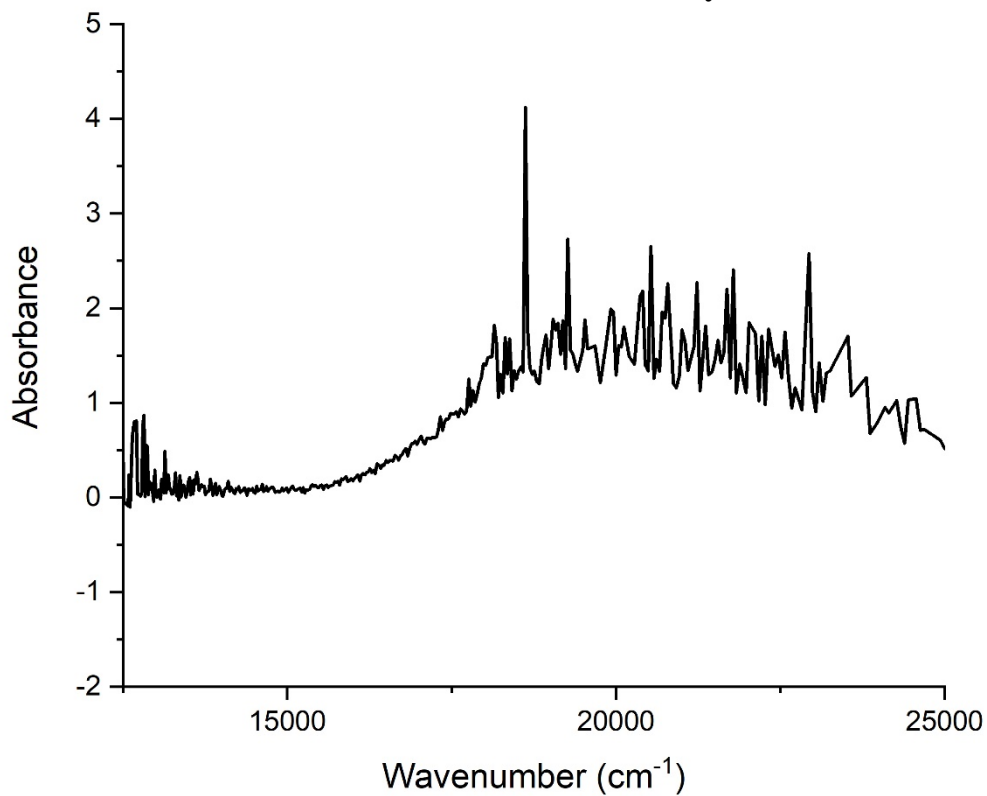**Information for Marcus-Hush Analysis of 2**

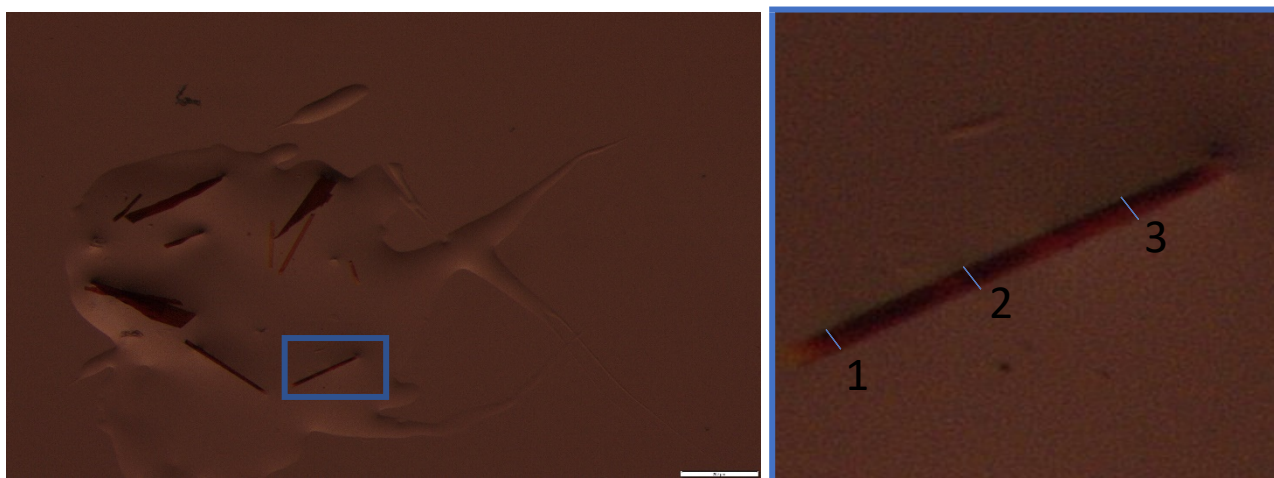**Figure S32: SC-UV-Vis spectrum of 2 from horizontally polarised light**

Figure S33: Crystal images of 2 used to measure the width of the crystal
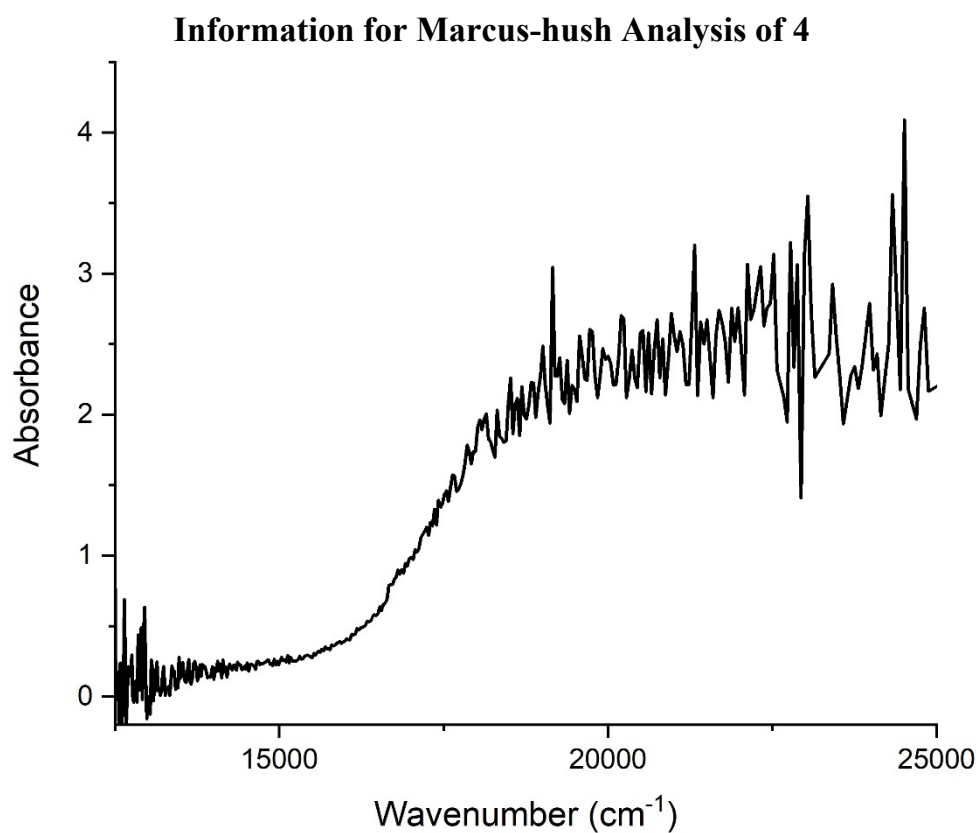
1: 15.443 pixels 2: 13.463 pixels 3: 14.151 pixels Av. Width = 14.352 pixels

200 μm scale bar: 255.666 therefore 0.782 pixels/μm

Crsytal width μm = 14.352 x 0.782 = 11.224 μm = 0.011224 mm = 0.0011224 cm

Table S8: Spectral data for 2

v_{max} (cm^{-1})*	F(R)$_{max}$ (a.u.)	$\Delta v_{1/2}$ (cm^{-1})	$\Delta v_{1/2}$° (cm^{-1})	ε (M^{-1} cm^{-1})	H$_{ab}$ (cm^{-1})
6213(20)	0.067(6)	543(51)	1051	19(4)	44(7)
6632	0.10	697	1269		
7127	0.07	1146	1627		
8016	0.12	4236	3128		
10828	0.15	1782	2028		
14881	0.49	1569	1903		
16637	1.24	1714	1990		
17868	1.79	2525	2415		
19662	1.59	3023	2643		
24802	5.34	8584	4453		

Information for Marcus-hush Analysis of 4

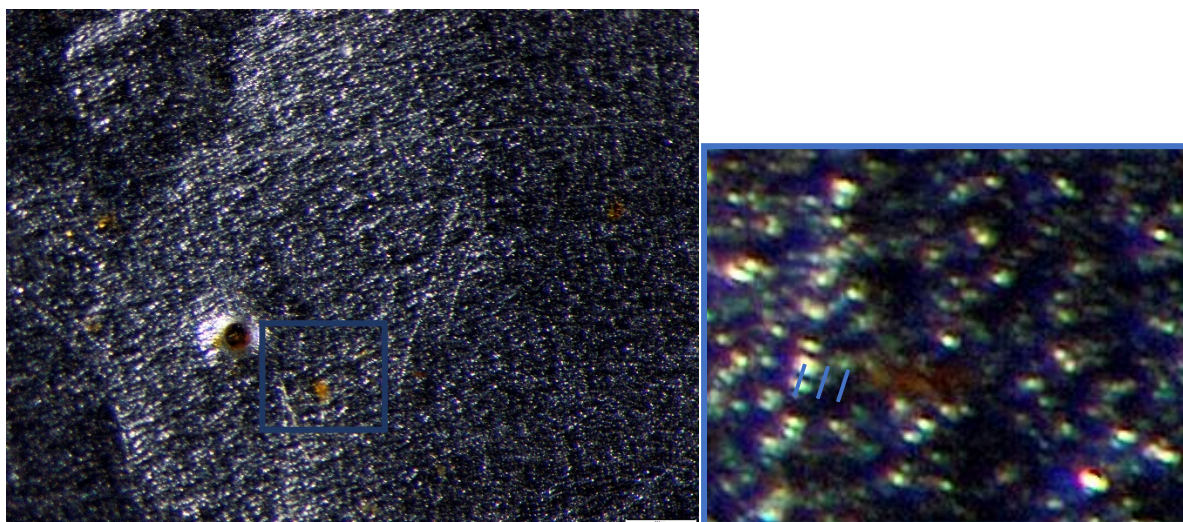**Figure S34: SC-UV-Vis spectrum of 4 from horizontally polarised light**

Figure S35: Crystal images of 4 used to measure the width of the crystal.

1: 16.125 pixels 2: 14.000 pixels 3 : 15.133 pixels Av width = 15.086 pixels

200 μm scale bar length = 256 pixels. 0.781 pixels/μm

Crystal width = 0.781 x 15.086 μm = 11.786 μm = 0.011786 mm = 0.0011786 cm

Table S9: Spectral data for 4

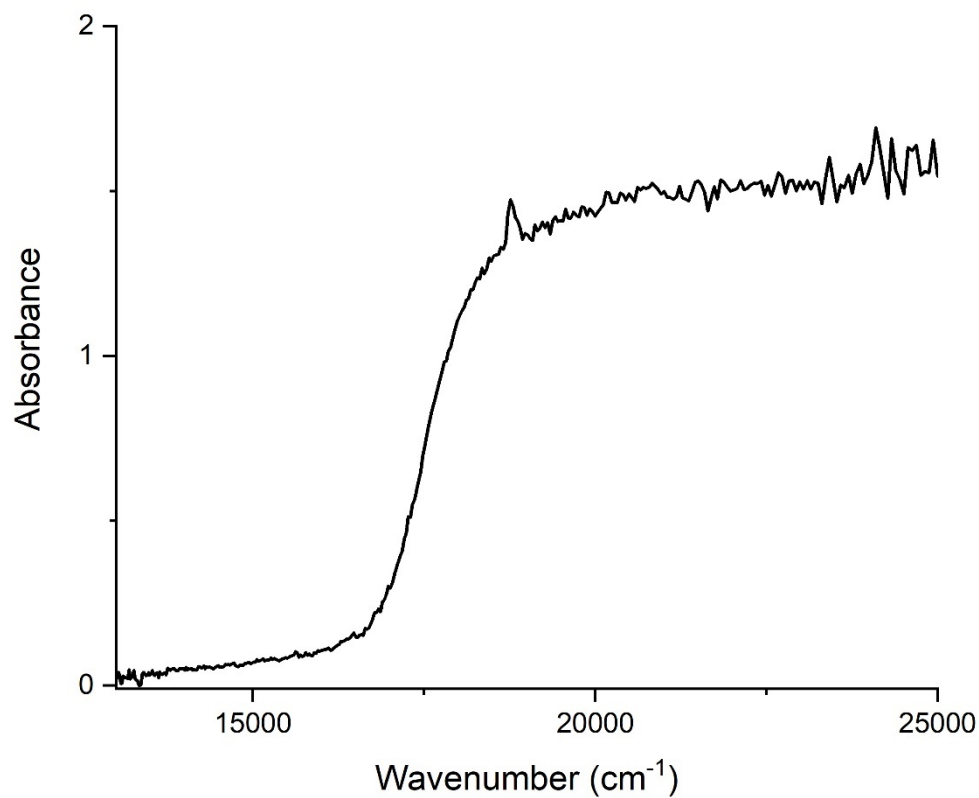| v_{max} (cm^{-1})*	F(R)$_{max}$ (a.u.)	$\Delta v_{1/2}$ (cm^{-1})	$\Delta v_{1/2}$° (cm^{-1})	ε (M^{-1} cm^{-1})	H$_{ab}$ (cm^{-1})
6616(19)	0.37(6)	945(10)	1472	67(11)	110(14)
7441	0.458	2023	2162		
10582	0.165	2217	2263		
15207	2.38	1836	2059		
18302	3.13	3746	2941		
23827	8.34	7665	4207		

Information for Marcus-Hush Analysis of 3

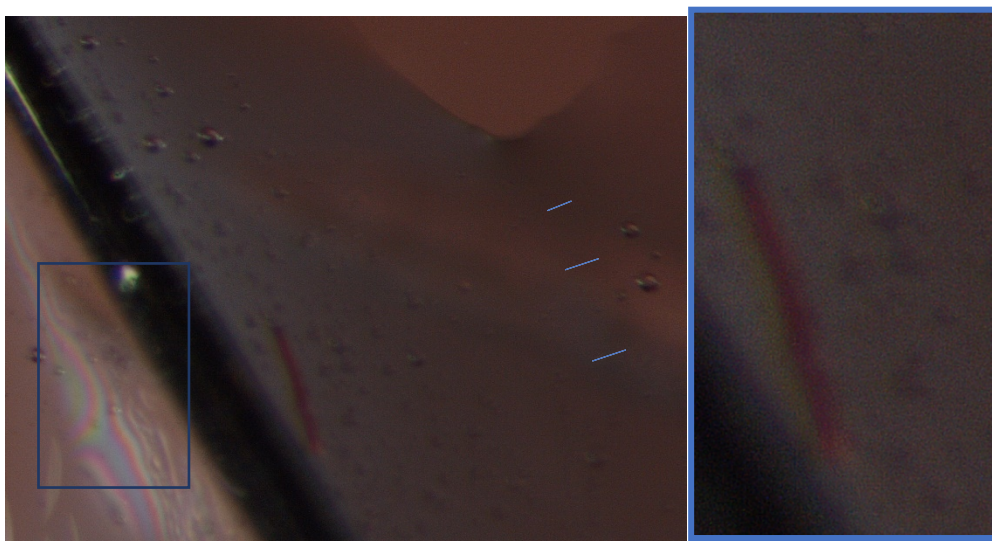**Figure S36: SC-UV-Vis spectrum of 3 from horizontally polarised light**

Figure S37: Crystal images of 3 used to measure the width of the crystal.

1: 20.881 pixels 2: 21.190 pixels 3 : 17.464 pixels Av width = 19.845 pixels

200 μm scale bar length = 254 pixels. 0.787 pixels/μm

Crystal width = 0.787 x 19.845 μm = 15.626 μm = 0.015626 mm = 0.0015626 cm

Table S10: Spectral data for 3

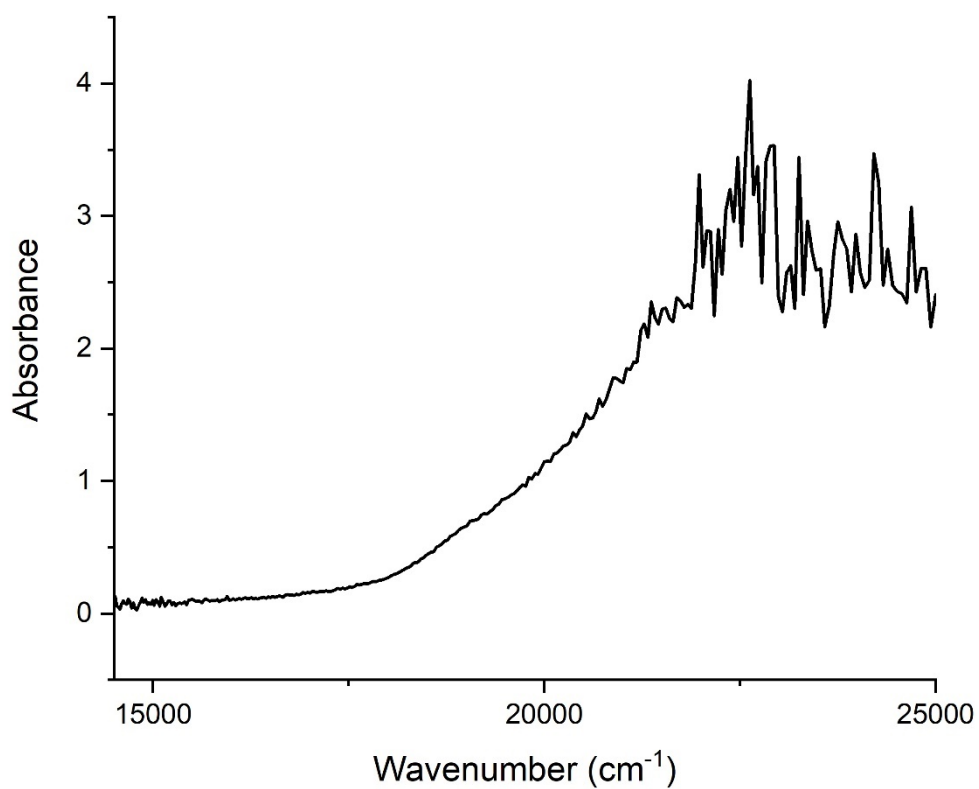| v_{max} (cm^{-1})*	F(R)$_{max}$ (a.u.)	$\Delta v_{1/2}$ (cm^{-1})	$\Delta v_{1/2}^{o}$ (cm^{-1})	ε (M^{-1} cm^{-1})	H$_{ab}$ (cm^{-1})
6051(97)	0.12(1)	862(137)	3778	37(4)	75(11)
6670(127)	0.215(7)	1224(208)	3973		
7383(141)	0.13(5)	1885(298)	4175		
11051	0.0442	811	5052		
14392	1.2755	2244	5765		
18296	2.49498	5326	6501		
24519	4.01606	7356	7525		

Information for Marcus-Hush Analysis of 3E

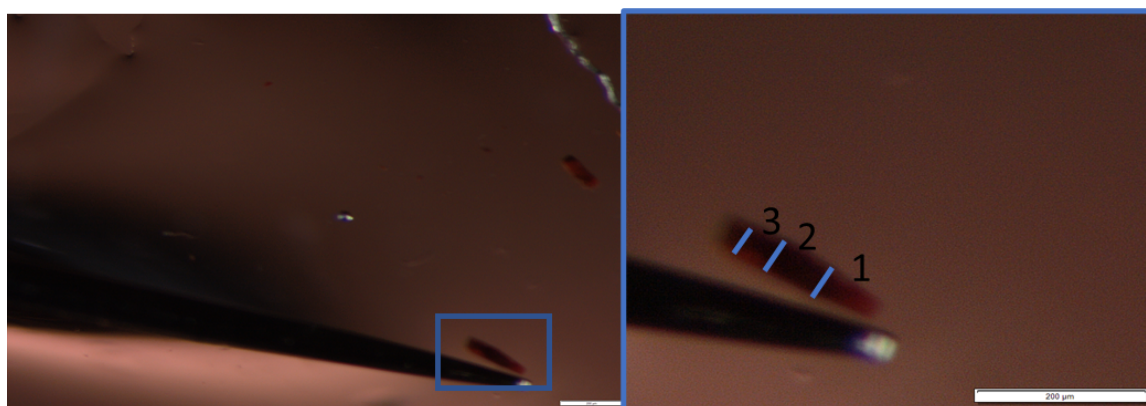**Figure S38: SC-UV-Vis spectrum of 3E from horizontally polarised light**

Figure S39: Crystal images of 3E used to measure the width of the crystal.

1: 30.30 pixels 2: 19.063 pixels 3: 20.436 pixels Av width = 23.26 pixels

200 μm scale bar length = 253 pixels. 0.79 pixels/μm

Crystal width = 0.79 x 23.26 μm = 18.375 μm = 0.018375 mm = 0.0018375 cm

Table S11: Spectral data for 3E

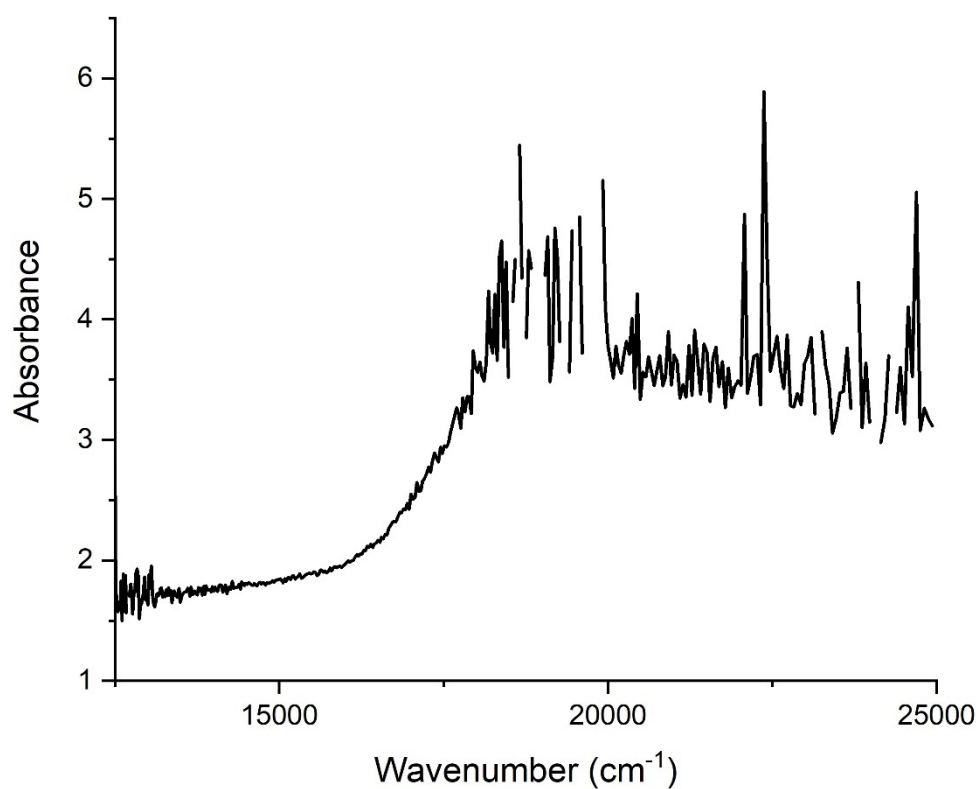| v_{max} (cm⁻¹)*	$F(R)_{max}$ (a.u.)	$\Delta v_{1/2}$ (cm⁻¹)	$\Delta v_{1/2}^{o}$ (cm⁻¹)	ε (M⁻¹ cm⁻¹)	H_{ab} (cm⁻¹)
6945(127)	0.1152(0.06)	2567(137)	4005.365	35(20)	136(46)
7690	0.11921	2370	4214.724		
9264	0.45257	1513	4625.996		
10100	0.79299	1108	4830.217		
14853	4.46822	3893	5857.511		
19103	1.65525	3333	6642.886		
24666	5.31622	9007	7548.408		

Information for Marcus hush analysis of 1E

Figure S40: SC-UV-Vis spectrum of 1E from horizontally polarised light

Figure S41: Crystal images of 1E used to measure the width of the crystal

Scale bar length 100 micron= 102.044 pixels 0.980 microns/pixel

3 measurements from crystal 1. 32.242 pixels 2. 30.594 pixels 3. 31.048 pixels av = 31.294

Crystal width = 30.67 microns. = 0.03067mm = 0.003067 cm

Table S12: Spectral data for 1E

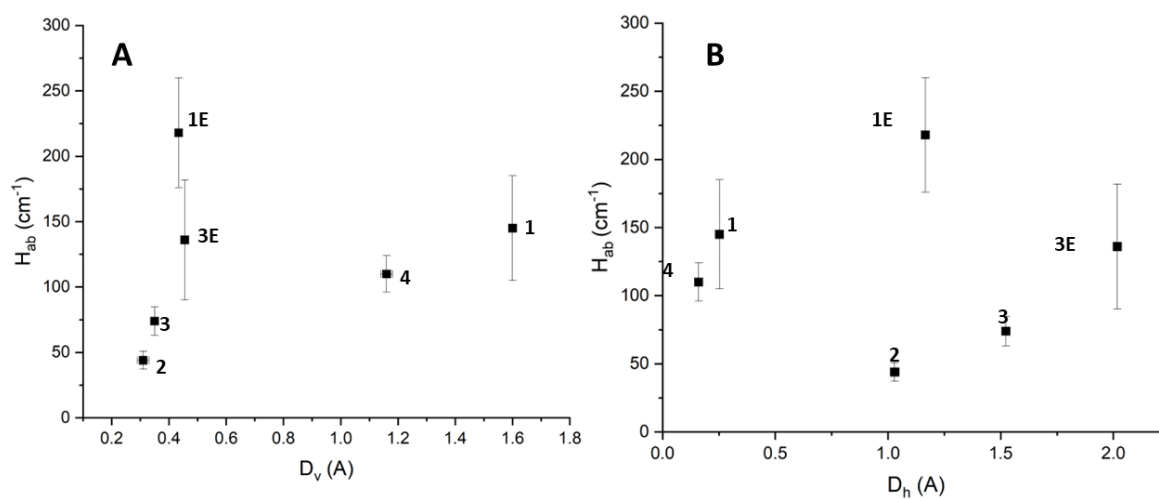| v_{max} (cm^{-1})*	F(R)$_{max}$ (a.u.)	$\Delta v_{1/2}$ (cm^{-1})	$\Delta v_{1/2}^{o}$ (cm^{-1})	ε (M^{-1} cm^{-1})	H$_{ab}$ (cm^{-1})
6012(33)	0.27(0.06)	1313(97)	1791	205(60)	218(42)
7377	0.25469	1437	1821		
9458	1.13392	2608	2454		
10671	0.68029	1333	1754		
14996	0.98449	2180	2244		
15197	0.28727	5509	3567		
24279	1.22883	9993	4804		

Additional Structure-Activity Relationship Plots

Figure S42: Effect of vertical (B) and horizontal (A) offsets on the H$_{ab}$ of the low energy IVCT transition.

Table S13: Compiled SEC-UV-Vis data as was used for the H_{ab} calculation

	6000 cm^{-1} IVCT transition						10,000 cm^{-1} IVCT transition					
	1	1E	2	3	3E	4	1	1E	2	3	3E	4
Crystal Width (cm)	0.0013 ± 0.0001	0.00283 ± 0.0004	0.00112 ± 0.00007	0.0016 ± 0.0001	0.0018 ± 0.0002	0.00118 ± 0.00008	0.0013 ± 0.0001	0.00283 ± 0.0004	0.00112 ± 0.00007	0.0016 ± 0.0001	0.0018 ± 0.0002	0.00118 ± 0.00008
SC-UV-Vis Absorbance	2.18 ± 0.48	4.22 ± 0.54	1.59 ± 0.33	2.36 ± 0.27	1.49 ± 0.04	2.6 ± 0.4	2.18 ± 0.48	4.22 ± 0.54	1.59 ± 0.33	2.36 ± 0.27	1.49 ± 0.04	2.6 ± 0.4
v_{max} (cm^{-1})	6479 ± 178	6012 ± 33	6213 ± 20	6616 ± 19	6051 ± 97	6945 ± 127	9999 ± 242	9793 ± 259	10521 ± 58	10538 ± 149	10427 ± 92	9682 ± 127
$F(R)_{max}$	0.33 ± 0.09	0.27 ±0.06	0.067 ± 0.006	0.37 ± 0.06	0.12 ±0.01	0.1152 ± 0.0576	0.677 ± 0.22	0.86 ±0.25	0.33 ± 0.01	0.313 ± 0.06	0.49 ±0.07	0.68 ±0.05
$\Delta v_{1/2}$ (cm^{-1})	1221 ± 165	1313 ± 97	543 ± 51	945 ± 10	862 ± 137	2567 ± 137	1876 ± 260.5	2156 ± 370	1778 ± 597	1397 ± 278	1844 ± 740	2302 ± 137
SC-UV-Vis ε	1074 ± 321	1753 ± 478	1000 ± 271	1136 ± 208	1035 ± 93	1128 ± 303	1074 ± 321	1753 ± 478	1000 ± 271	1136 ± 208	1035 ± 93	1128 ± 302
IVCT ε (mol^{-1}L^{-1}cm^{-1})	91 ± 34	222 ± 69	19 ± 4	67 ± 16	37 ± 4	35 ± 20	248 ± 78	653 ± 228	91 ± 14	68 ± 18	150 ± 26	209 ± 41
Cofacial Distance (Å)	3.782 ± 0.004	3.318 ± 0.004	3.9 ± 0.6	3.78 ± 0.005	3.482 ± 0.003	3.45029 ± 0.00013	3.782 ± 0.004	3.318 ± 0.004	3.9 ± 0.6	3.78 ± 0.005	3.482 ± 0.003	3.45 ± 0.0001
H_{ab} (cm^{-1})	145 ± 40	227 ± 47	44 ± 7	110 ± 14	75 ± 11	136 ± 46	321 ± 97	637 ± 177	221 ± 53	171 ± 41	291 ± 86	370 ± 51

Crystal width is the measured width of each of the crystals under a light microscope. SC-UV-Vis absorbance is the measure absorbance from the single crystal UV-Vis experiment. v_{max} is the peak position of the IVCT band of interest. $F(R)_{max}$ is the maximum observed absorbance for the IVCT band of interest. $\Delta v_{1/2}$ is the full width at half maximum for the IVCT band of interes. SC-UV-Vis ε is the absorption coefficient calculated from the single crystal UV-Vis experiment. IVCT ε is the adjusted absorption coefficient adjusted to correspond to the IVCT band of interest. Cofaical distance is the distance between interacting TTF groups as measured in OLEX. $H_{ab} = [0.0205 \times (v_{max} \varepsilon \Delta v_{1/2}) \, 1/2]/r$, where ε is the extinction coefficient of the IVCT band.
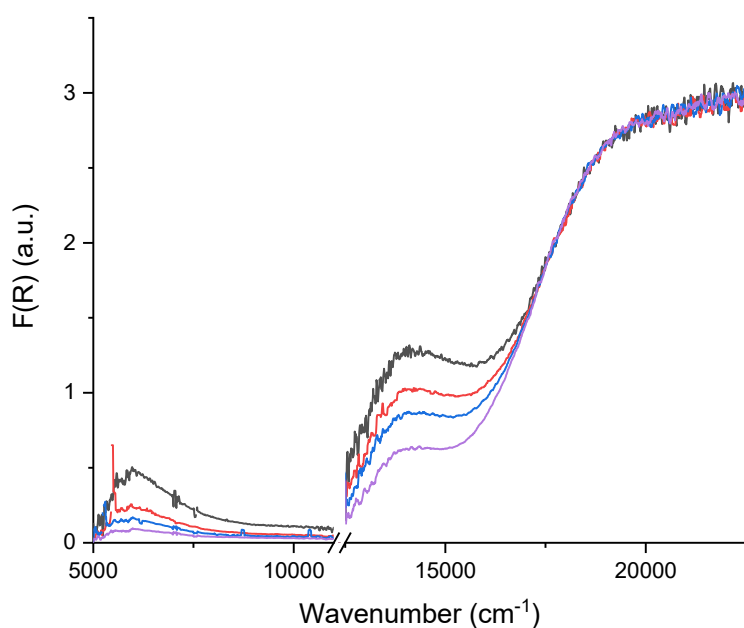
Figure S43: UV-Vis spectrum of 1E after the oxidising potential has been removed for 90 s (black), 180 s (red), 270 s (blue), and 450 s (purple).
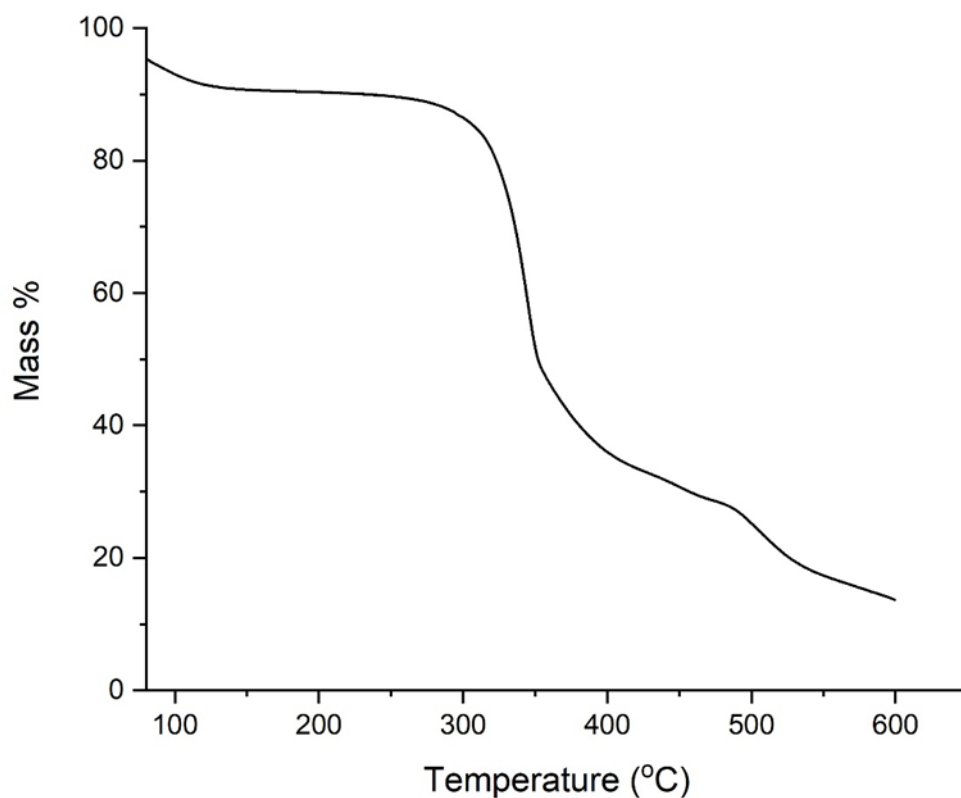

Figure S44: TGA decomposition curve of Framework 1. Data was collected under an N_2 flow of 20 mLmin^{-1} at a scan rate of 5 °Cmin^{-1}.
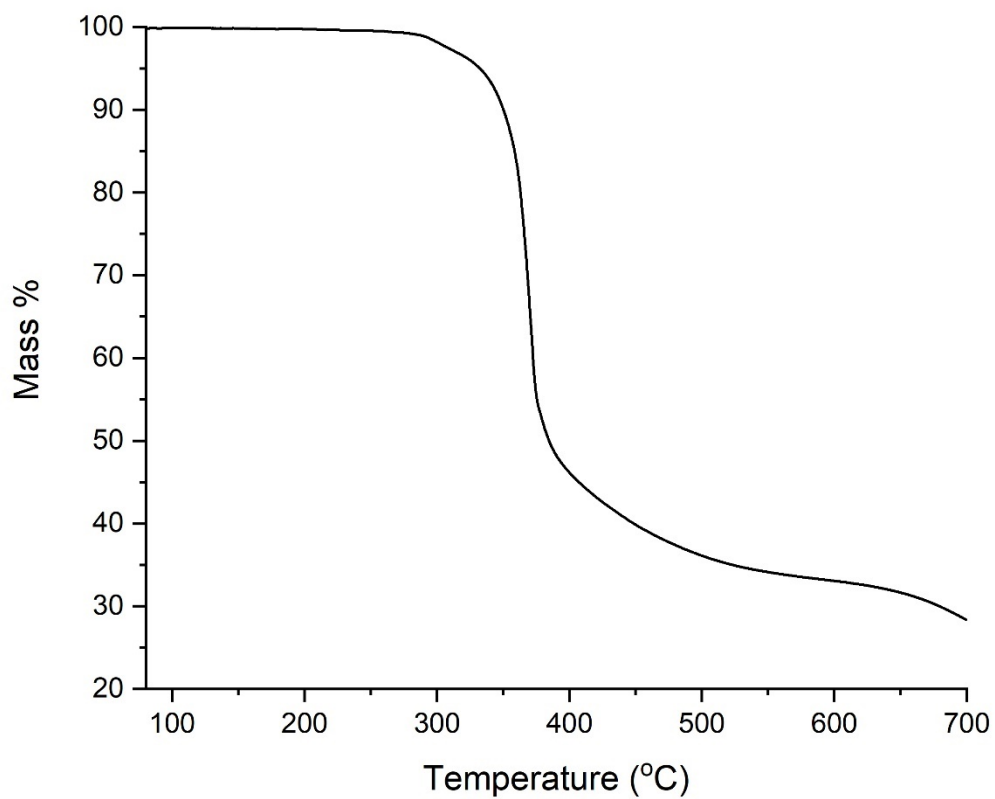
Figure S45: TGA decomposition curve of Framework 1E. Data was collected under an N$_2$ flow of 20 mLmin^{-1} at a scan rate of 5 °Cmin^{-1}.
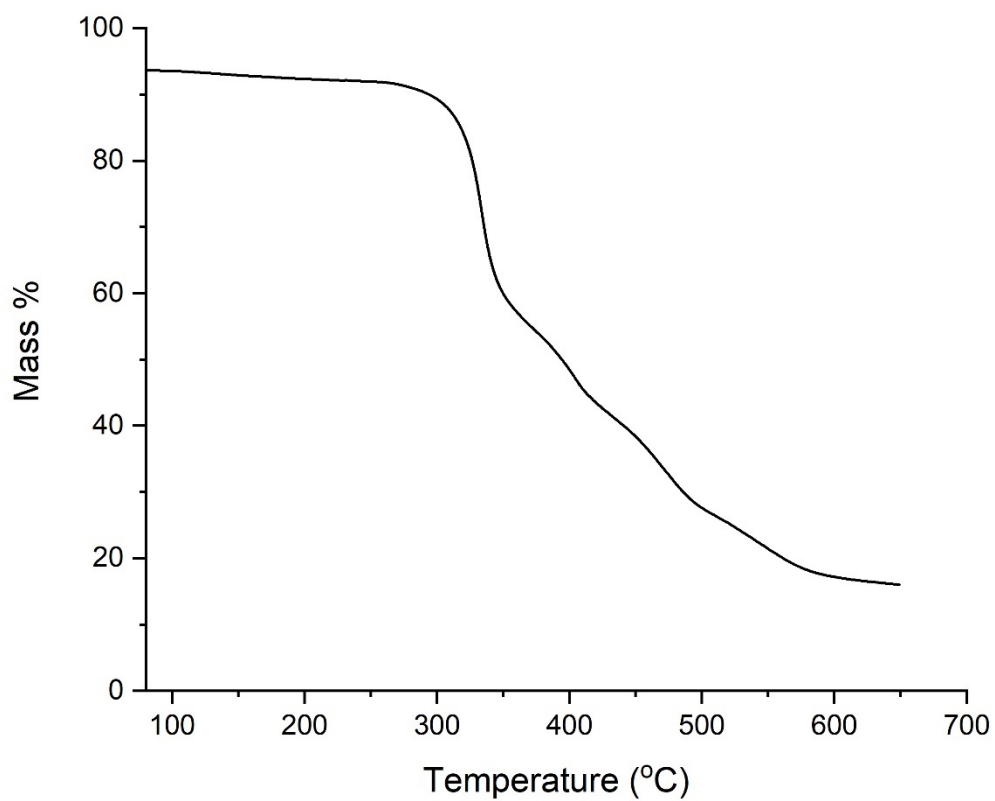

Figure S46: TGA decomposition curve of Framework 2. Data was collected under an N$_2$ flow of 20 mLmin^{-1} at a scan rate of 5 °Cmin^{-1}.
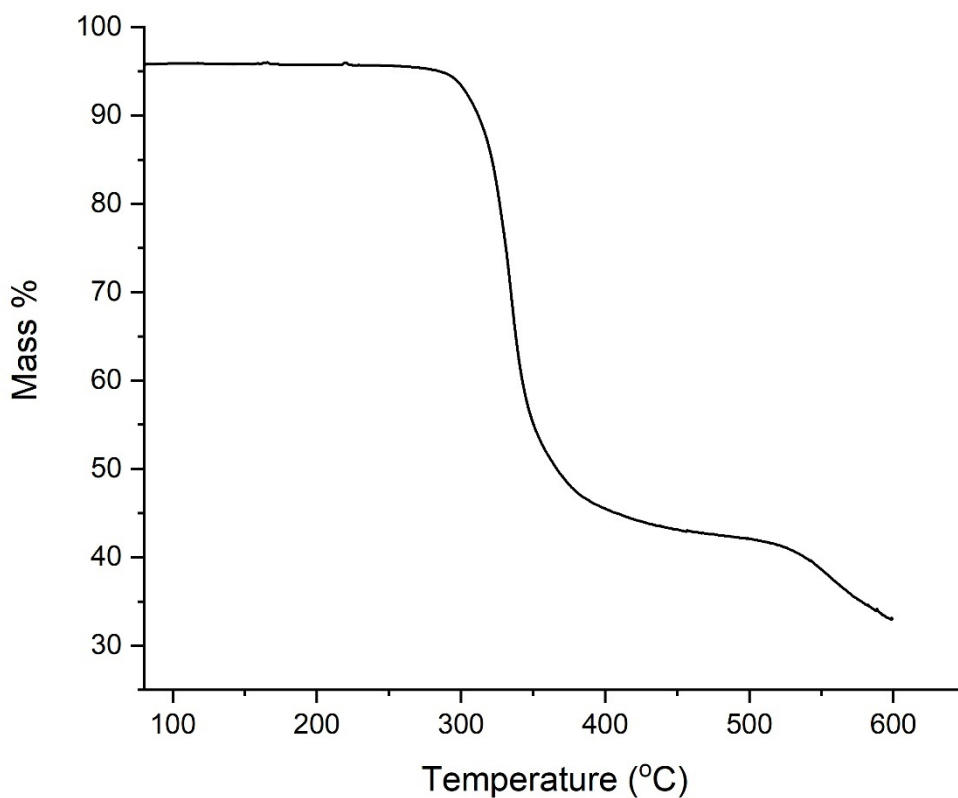
Figure S47: TGA decomposition curve of Framework 3. Data was collected under an N$_2$ flow of 20 mLmin^{-1} at a scan rate of 5 °Cmin^{-1}.
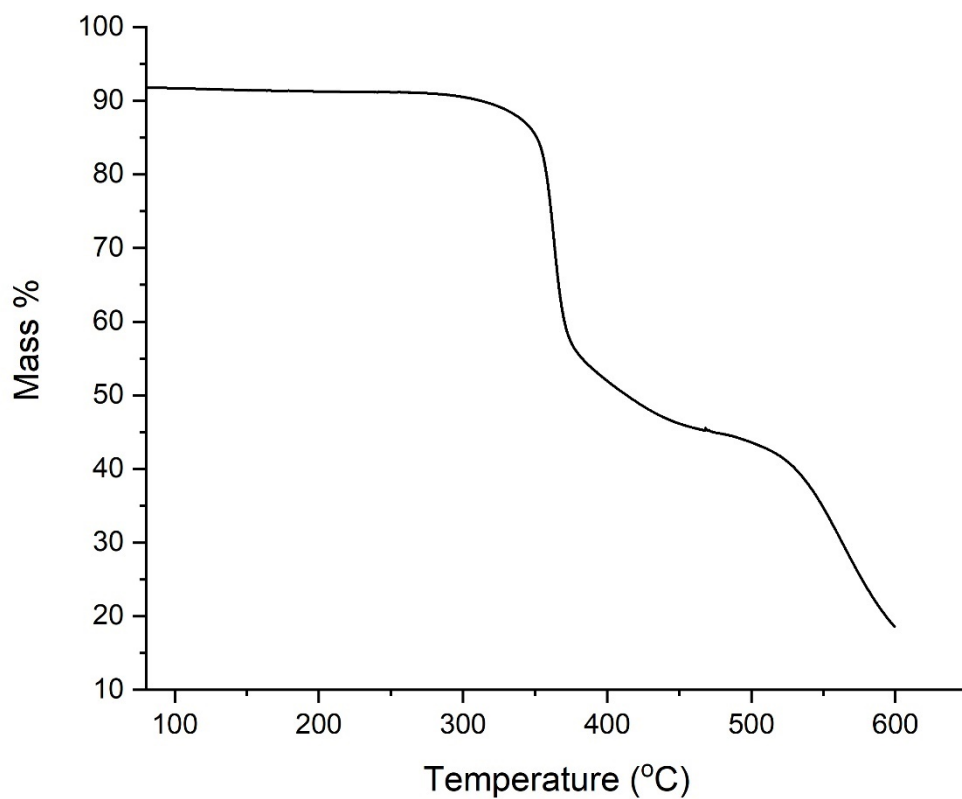

Figure S48: TGA decomposition curve of Framework 3E. Data was collected under an N$_2$ flow of 20 mLmin^{-1} at a scan rate of 5 °Cmin^{-1}.
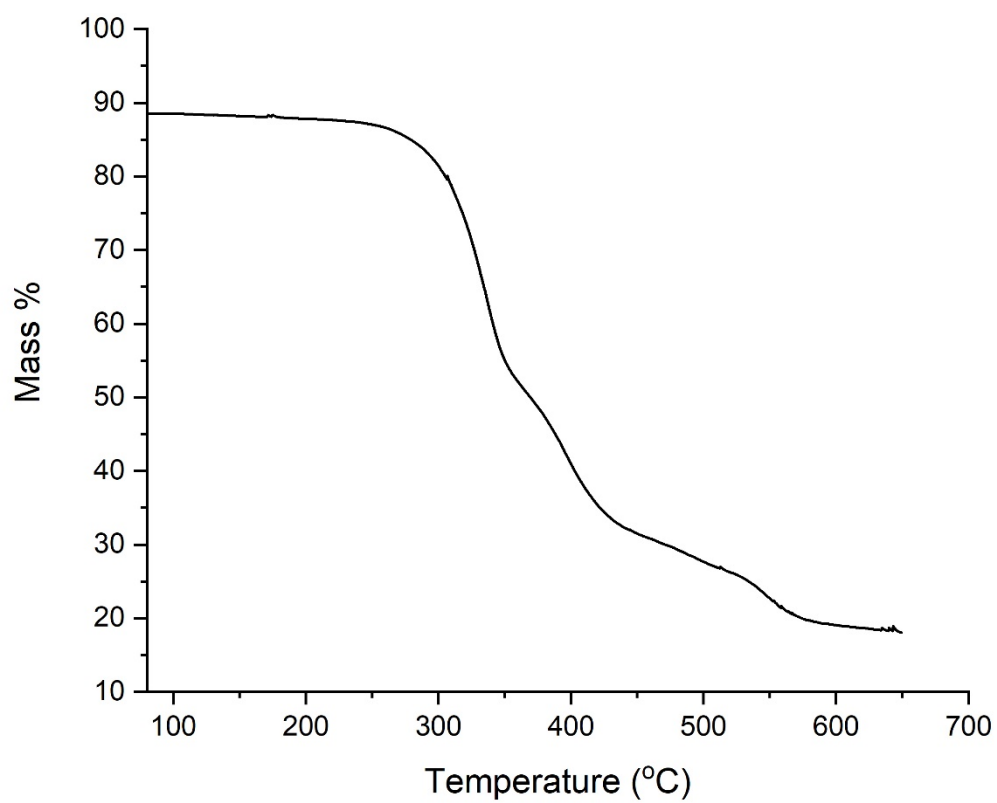
Figure S49: TGA decomposition curve of Framework 3E. Data was collected under an N$_2$ flow of 20 mLmin^{-1} at a scan rate of 5 °Cmin^{-1}.